Journal of Sound and Vibration 358 (2015) 152–175

Contents lists available at ScienceDirect

Journal of Sound and Vibration

journal homepage: www.elsevier.com/locate/jsvi

Review

An evaluation of displacement-based finite element models used for free vibration analysis of homogeneous and composite plates

V.N. Burlayenko [a,*], H. Altenbach [b], T. Sadowski [c]

[a] National Technical University 'Kharkiv Polytechnic Institute', Department of Applied Mathematics, 21 Frunze Str., 61002 Kharkiv, Ukraine
[b] Otto-von-Guericke University of Magdeburg, Lehrstuhl für Technische Mechanik, 2 Universitätsplatz, 39106 Magdeburg, Germany
[c] Lublin University of Technology, Department of Solid Mechanics, 40 Nadbystrzycka Str., 20-168 Lublin, Poland

ARTICLE INFO

Article history:
Received 31 March 2015
Received in revised form
4 August 2015
Accepted 6 August 2015
Handling Editor: M.P. Cartmell
Available online 29 August 2015

ABSTRACT

The finite element vibration analysis of plates has become one of the classical problems over the past several decades. Different finite element plate models based on classical, standard and improved shear deformable plate theories, three-dimensional elasticity equations or their combinations have been developed. The ability and accuracy of each such model can be established by validating it against analytical models, if it is possible, or other numerical models. In this paper, a comparative study of different plate finite element models used for the free vibration analysis of homogeneous isotropic and anisotropic, composite laminated and sandwich thin and thick plates with different boundary conditions is presented. The aim of the study is to find out the weaknesses and strengths of each model used and to pick out their interchangeability for the finite element calculations. For comparisons, the plate models based on classical and first-order shear deformation theories within the framework of both single-layer and layer-wise concept and three-dimensional theory of elasticity are used. The models are created using the finite element package ABAQUS$^{\mathrm{TM}}$. Natural frequencies obtained by the authors are compared with results known in the literature from different analytical or approximate solutions and, then, the correlation between them is discussed in detail. At the end, conclusions are drawn concerning the utility of each model considered for vibration predictions of plates.

Contents

* Corresponding author.
E-mail addresses: burlayenko@yahoo.com (V.N. Burlayenko), holm.altenbach@ovgu.de (H. Altenbach), t.sadowski@pollub.pl (T. Sadowski).

http://dx.doi.org/10.1016/j.jsv.2015.08.010

1. Introduction

Flat panels as design components have found applications in diverse fields of engineering, ranging from civil to aeronautical industries. Because of this, much research has been devoted to develop effective analysis tools that may combine easy usage and accurate predictive capability for evaluating their structural behavior. The vibration analysis of panels dealing with predictions of natural frequencies and associated mode shapes is among significant research activities in that sense. A good understanding of the free vibration behavior is of crucial importance toward reliable predictions of the dynamic response of plate-like structures to time-dependent external excitations and for their optimal design from the vibrational point of view.

The vibration analysis of plates has become one of the classical problems that researchers have been studying for over a century. In this respect, different methods including analytical, semi-analytical and numerical approaches have been developed. The most popular among them are Rayleigh–Ritz, Kantorovich, superposition-Galerkin, Navier and Lévy techniques as well as finite difference, differential quadrature, finite strip, finite element, boundary element methods, etc. A review of this topic can be found in various books and monographs, e.g. [1,2] among many others. Nevertheless, most significant advances in vibrational modelling have been achieved by using the finite element method (FEM) due to its great versatility and powerful capacity in solving multi-field tasks with complex geometry, boundary and loading conditions. Herewith, a large number of finite element (FE) models have been developed by using appropriate plate theories, which, in essence, are based on the through-the-thickness approximations of three-dimensional (3-D) displacement and stress fields and have been developed either within the non-polar theory of linear elasticity [3] or using the hypotheses of the Cosserat continuum [4]. Moreover, for flat panels made of modern composite materials, the plate theories developed can be applied within the framework of either equivalent single-layer (ESL) or layer-wise (LW) concepts [5]. Some of the most relevant and several recent works about finite element free vibration analysis of plates are mentioned below.

The first important contribution into the analysis of thin plates was the theory developed by Kirchhoff that is referred now as the classical plate theory (CPT). A detailed literature search revealed that the FE models of plates employing the assumptions of the CPT are accurate to analyze flexural vibrations of thin homogeneous plates, as shown in [6,7] and give only acceptable results for laminated thin plates, defined within the ESL concept, as presented in [8,9]. Besides, it was recognized, e.g. in [10] that the CPT, neglecting transverse shear deformations results in an overestimation of natural frequencies for moderately thick homogeneous and composite plates.

To overcome the limitations of the classical theory, the first-order shear deformation theory (FSDT) of plates based on the Reissner or Mindlin assumptions is commonly used. The literature overview showed that the FE models based on the FSDT for studying the free vibration problem give sufficiently accurate results for homogeneous isotropic and anisotropic thick plates, e.g. in [11,12] and provide an adequate description of the shear deformability of composite plates, which are modelled as one-layer structures within the ESL approach, e.g. in [13,14]. Although these FE models are used in conjunction with assumptions on the shear correction factor [15], upon which the accuracy of prediction with FSDT is very sensitive, many researchers have found that FE models based on the Reissner–Mindlin finite element exhibit a shear-locking effect in situations, when the plate thickness decreases. To avoid this parasitic effect and to keep advantages of the FSDT were suggested different correction techniques, e.g. the reduced integration or selective integration schemes [16] as well as different FE formulations such as an assumed-strain finite element, e.g. in [17].

Aiming to include partially or completely through-the-thickness C^0 requirements in the FE formulation of layered plates and to avoid the calculation of shear correction coefficients, finite elements based on the high-order shear deformation theories (HSDT) have been also developed, e.g. in [18,19] for homogeneous thick plates and in [20–22] for laminated plates assuming their single-layered structure within the ESL. According to the HSDT, the initial assumptions on the high order of displacement polynomials do not lead to a constant shear stress distribution through the thickness and therefore the artificial shear correction factor is not involved in analysis of composite laminated and sandwich plates [23]. Moreover, these elements are free from locking phenomena. Nevertheless, the use of such finite elements is limited because they

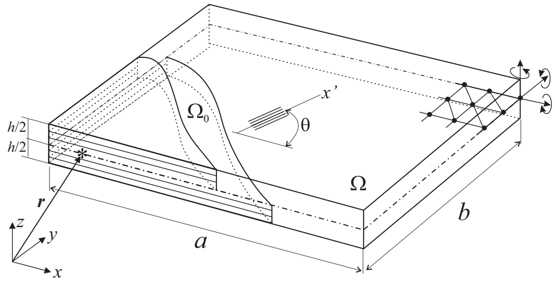

Fig. 1. Geometry of laminated composite plate.

require C^1 continuity in their FE formulations that is not simple to obtain for generalized finite elements [24]. Assumed strain finite element based on Reddy's HSDT has been also developed to analyze free vibrations and buckling of composite plates, e.g. in [25,26]. Recently, new sophisticated HSDTs have been proposed and applied for the free vibration analysis of composite laminated and sandwich plates, e.g. in [27–29]. It should be mentioned that any HSDT has to be proved with respect to the consistency demands as formulated, e.g. in [30].

Applying the equations of elasticity theory to a single-layer FE model of a plate is attractive for investigations of free vibrations of homogeneous thick and composite laminated plates as shown in [31–33] and [31,34,35], respectively. However, due to complexities in the FE formulation and difficulties in providing accurate boundary conditions corresponding to the same 2-D plate models as well as a very high computational cost in comparison with the 2-D plate models have made 3-D FE models rarely used in FE modelling. Alternatively, continuum-based (or degenerated) plate/shell finite elements developed by discretizing the 3-D elasticity equations in terms of mid-surface nodal variables [36] have gained a wide application for the FE modal analysis of thick homogeneous and composite plates. For example, in [37] the free vibration of isotropic plates and shells has been studied with a nine-node degenerated shell element, whereas in [38] this element was exploited for the free vibration of laminated plates.

The discrete layer-wise concept is potentially accurate for both displacements and transverse stress and strain predictions in the case of composite plates with ply stacking sequences through the thickness. Consequently, such FE models provide a correct representation of dynamic flexural behavior of laminated and sandwich plates, e.g. [39,40] and more recently [41–43] among others. The disadvantage of discrete layer plate elements is connected with a huge number of nodal unknowns and, as a result, a significant computational cost, which increases in direct proportion to the increasing number of laminas. Thereby, although layer-wise FE models may be effective for predicting interlaminar properties of plates in dynamic analysis, e.g. in [44,45], the high computational cost restricts their wide usage for many practical applications.

Significant improvements in the interlaminar response of laminated plate models without introducing additional kinematic variables have been achieved by using a piece-wise linear (zig-zag) approximation of the in-plane displacements through the laminate thickness [46]. Zig-zag FE models developed, for instance, in [47–49] for the free vibration analysis of multilayered composite plates were favored against the ones based on the discrete layer-wise approach. They can be considered as a reasonable compromise between accuracy and a low computational cost. However, finite elements based on this theory require either C^1 or even C^2 continuity in their formulation, and on the other hand each zig-zag function added to displacement components increases the number of degree of freedom (DOF) per node. Thereby, their implementation into general-purpose finite element codes becomes inconvenient.

Most recently, a series of new high-order sandwich panel theories (HSAPT) have been developed within the layer-wise concept to analyze three-layered sandwich plates with a flexible thick core, e.g. [50]. The main idea of the HSAPT is an introduction of the kinematic assumptions based on any of the plate theories for the face sheets, while the behavior of the core should be described by the equations of elasticity related to the plate equations through appropriate compatibility conditions. A comparison of free vibration predictions for sandwich plates, performed with the HSAPT and resulting from the use of the elasticity theory and experimental observations, has shown very good correlations between them [51,52]. Moreover, the HSAPT is suitable for analyzing debonding issue at the interface between the face sheet and the core in sandwich plates, as shown, e.g. in [53–55]. Similar ideas of using different plate models for different constituent layers within the layer-wise approach have been used for analyzing sandwich plates with flexible and thin cores in [56,57].

Due to growing interest in appropriate analysis tools, capable of carrying out effective and accurate modelling in conjunction with versatility and easiness in use, researchers more and more utilize commercial finite element codes in modern engineering practice. In this respect, notwithstanding the great amount of literature on the free vibration analysis of homogeneous and composite laminated and sandwich plates, in the authors' opinion there is a need to classify computational models based on the existing plate theories within their applicability to engineering tasks. This would allow an engineer to understand the clear limits in using those theories for making a rational compromise between the required precision of the analysis and computational costs. Hitherto, only a few papers have been devoted to comprehensive numerical comparisons of the plate theories used for the vibrational analysis. In [58], the assessment of the plate theories has been done without models based on layer-wise and three-dimensional approaches. The authors of [59] have presented a comparison of different plate models utilized mainly for a static analysis. An assessment of dynamic plate models within the framework of Carrera's Unified Formulation was performed in [60], however, the comparisons were limited by the case of simply supported plates only. Recently, comparisons between different shear deformation plate models used for the free vibration analysis of simply supported plates have been done in [61], while in [62] 3-D plate models and plates endowed by the FSDT have been compared for free vibration predictions.

With this in mind, numerical computations of natural frequencies and associated mode shapes of homogeneous isotropic and anisotropic, laminated and sandwich rectangular plates with a variety of length to thickness ratios, boundary conditions, lay-up sequences and core types, based on different FE models including CPT, FSDT within both the ESL and LW concepts, and 3-D finite elements developed with the ABAQUS^{TM} code [63] are presented in this paper. The obtained results are compared with those earlier published in the literature and, therefore, could be useful as a benchmark for researchers. The quantitative differences between FE models applied to the same plate are also discussed to show which one would be preferable for engineering design.

2. General displacement-based kinematic assumptions

As far as FE modelling is concerned given that this subject of this paper we briefly recall, using the standard matrix notations, the mentioned above two-dimensional Kirchhoff–Love, Reissner–Mindlin and common ideas of the high-order shear deformation plate theories.

Let us consider an arbitrary plate composed of, in general, a number of dissimilar material layers. We will suppose that along the thickness, the plate is divided into L sub-layers of constant thicknesses. The total domain Ω of the plate consists of the mid-surface Ω_0 and the thickness h. It should be noted that plates of constant thickness are only considered. The geometry and reference system are shown in Fig. 1 and can be defined as

$$\Omega=\left\{(x,y,z)|(x,y)\in\Omega_0, z\in\left[-\frac{h}{2},\frac{h}{2}\right]\right\} \tag{1}$$

In this paper we assume that the displacements are master fields. The slave fields are strains and stresses, which can be calculated by appropriate strain–displacement and stress–strain relations, respectively. Let the number of variables per node $\mathbf{q}_e$ of a finite element be determined by the kinematic assumptions imposed on the displacement field through the plate thickness:

$$\mathbf{u}=\mathbf{N}\mathbf{q}_e \tag{2}$$

where $\mathbf{u}=\{u(\mathbf{r},t),v(\mathbf{r},t),w(\mathbf{r},t)\}$ is a displacement vector of in-plane displacements and deflection of any particle in a multilayered plate located at Cartesian coordinate $\mathbf{r}(x,y,z)$, and $\mathbf{N}$ denotes shape functions associated with the considered element. The displacement components u, v and w are measured with respect to the plate reference surface Ω_0.

The displacement field within each ith layer $(i=1,\dots,L)$ is commonly assumed to be of the form

$$\mathbf{u}^i(\mathbf{r},t)=\mathbf{u}_0^i(\mathbf{r}_0,t)+\mathbf{U}^i(\mathbf{r},t) \tag{3}$$

where $\mathbf{u}_0^i=\{u_0^i(\mathbf{r}_0,t),v_0^i(\mathbf{r}_0,t),w_0^i(\mathbf{r}_0,t)\}$ is a displacement vector of a point in the reference surface, $\mathbf{U}^i=\{U^i(\mathbf{r},t),$ $V^i(\mathbf{r},t),W^i(\mathbf{r},t)\}$ is a vector of position functions and $\mathbf{r}_0=\mathbf{r}(x,y,0)$ is a location vector of the reference surface.

In order to reduce the initial 3-D presentation to a 2-D one, it should be assumed that the variation of $\mathbf{U}^i$ relative to the thickness coordinate z can be expected as the following linear combination:

$$\mathbf{U}^i(\mathbf{r},t)=\sum_{k=1}^{n}[\Phi_k^i(z)]\mathbf{U}_k^i(\mathbf{r}_0,t) \tag{4}$$

where $\mathbf{U}_k^i\{U_k^i(\mathbf{r}_0,t),V_k^i(\mathbf{r}_0,t),W_k^i(\mathbf{r}_0,t)\}$ is a vector of unknown coefficients and

$$[\mathbf{\Phi}_k^i(z)]=\begin{pmatrix}\phi_k^i(z) & 0 & 0\\ 0 & \phi_k^i(z) & 0\\ 0 & 0 & \varphi_k^i(z)\end{pmatrix} \tag{5}$$

is a matrix of continuous functions of the coordinate z, which satisfies the conditions: $\phi_k^i(0)=0$ and $\varphi_k^i(0)=0$, $k=1,2,\dots,n$.

Herewith, an appropriate selection of the coefficients and functions of the matrix $[\mathbf{\Phi}_k^i]$ allows for the derivation of various plate theories as special cases.

2.1. Classical Kirchhoff's model

In the Kirchhoff–Love theory of plates in bending it was assumed that the straight lines perpendicular to the undeformed reference surface remain straight and perpendicular to it after deformation [23]. The displacement field expressed by (4) may be written as

$$n=1,\quad \mathbf{U}_1^i=\left\{-\frac{\partial w_0}{\partial x},-\frac{\partial w_0}{\partial y},0\right\} \tag{6}$$

$$[\mathbf{\Phi}_1^i(z)] = \begin{pmatrix} z & 0 & 0 \\ 0 & z & 0 \\ 0 & 0 & 0 \end{pmatrix} \tag{7}$$

Linear and constant variations through the thickness of the in-plane and transverse displacement components result in zero transverse shear deformations. Moreover, from the six nodal kinematic variables $\mathbf{q}_e$, i.e. three reference-plane displacements and three rotations around the appropriate coordinate axes, the two rotations caused by the plate bending depend on the plate deflection.

2.2. Reissner–Mindlin's first-order shear deformation model

Reissner-Mindlin theory assumes that the straight lines, which are perpendicular to the reference surface before deformation, remain straight but not necessarily perpendicular after deformation [23]. Thus, the line is permitted to rotate relative to the normal of the reference surface. Hence, the displacement field can be obtained by accepting the following setting in (4):

$$n = 1, \quad \mathbf{U}_1^i = \{\vartheta_x, \vartheta_y, 0\} \tag{8}$$

$$[\mathbf{\Phi}_1^i(z)] = \begin{pmatrix} z & 0 & 0 \\ 0 & z & 0 \\ 0 & 0 & 0 \end{pmatrix} \tag{9}$$

Here $\vartheta_x(x, y, t)$ and $\vartheta_y(x, y, t)$ are the independent rotations of a normal to the reference surface with respect to x and y axes. The inclusion of the independent bending rotations results in an average account of transverse shear deformation, thus discarding the zero transverse shear assumption dictated by the classical Kirchhoff–Love hypothesis. The strains and curvatures are expressed in terms of the first gradients of the kinematic variables, thus permitting simple C^0-continuous finite element approximations for these variables. Nevertheless, Reissner–Mindlin theory derived directly from the displacement field yields a constant value of transverse shear strains and constant value of shear stresses through the thickness. To account for the discrepancy between the strain energy of shear deformations caused by their constant state in the FSDT theory and of their parabolic distribution in the elasticity theory, a shear correction factor is needed. In essence, these factors are problem dependent [15,64].

2.3. Refined and layer-wise models

Refined shear deformation theories, based on series expansions of the displacement field in term of the plate thickness coordinate, truncated at a required order of this coordinate, can be expressed by Eq. (4), choosing the appropriate matrices within it. For instance, the well-known third-order shear deformation theory developed in [20] can be presented in this unified manner as follows:

$$n = 3, \quad \mathbf{U}_1^i = \{\vartheta_x, \vartheta_y, 0\}, \quad \mathbf{U}_2^i = \{\varphi_x, \varphi_y, 0\} \quad \text{and} \quad \mathbf{U}_3^i = \{\psi_x, \psi_y, 0\} \tag{10}$$

$$[\mathbf{\Phi}_1^i(z)] = \begin{pmatrix} z & 0 & 0 \\ 0 & z & 0 \\ 0 & 0 & 0 \end{pmatrix}, \quad [\mathbf{\Phi}_2^i(z)] = \begin{pmatrix} z^2 & 0 & 0 \\ 0 & z^2 & 0 \\ 0 & 0 & 0 \end{pmatrix} \text{and} \quad [\mathbf{\Phi}_3^i(z)] = \begin{pmatrix} z^3 & 0 & 0 \\ 0 & z^3 & 0 \\ 0 & 0 & 0 \end{pmatrix} \tag{11}$$

Here, the displacement components $\vartheta_x, \vartheta_y, \varphi_x, \varphi_y, \psi_x, \psi_y$ are unknown functions of position (x,y) and time t, as presented in [20].

Moreover, the value $i = 1$ means that single displacement expansions through the thickness of a multilayered plate (equivalent single-layer approach) is used, and $i > 1$ corresponds to the layer-wise approach assuming independent displacement variables in each layer. In this case, additional continuity conditions at the layer interfaces must be imposed on the functions in (4) such that the displacements must be continuous, but, in general, their derivatives with respect to z can be either discontinuous or continuous. Also zero transverse shear stresses on the bottom and top plate surfaces and their continuity in the thickness direction should be fulfilled too. A detailed discussion of the available refined shear and layer-wise theories as well as layer independent layer-wise theories using opportune zig-zag functions is out of the scope of this paper and can be found elsewhere, e.g. in [23].

3. Finite element statement

The mathematical aspects of a general finite element statement of plate/shell problems are widely discussed and presented in enormous number of publications. Thus, in the present paper only a brief formulation of this problem to the extent that is needed just for basic FE procedures used is given below.

3.1. The system of equations of motion

The principle of virtual work (PVW) presents the starting point of a FE formulation. We confine our analysis to free vibrations. Then, according to standard finite element notations [16], when the total plate domain Ω is discretized into NE finite elements (Fig. 1), one can write the equilibrium between the elastic internal and inertial forces within each finite element as follows:

$$\delta A_{\text{int}} + \delta A_{\text{inr}} = 0 \tag{12}$$

Here, the internal and inertial works done by those forces can be expressed as

$$\delta A_{\text{int}} = \delta \mathbf{q}_e^T \mathbf{K}_e \mathbf{q}_e \quad \text{and} \tag{13}$$

$$\delta A_{\text{inr}} = \delta \mathbf{q}_e^T \mathbf{M}_e \ddot{\mathbf{q}}_e \tag{14}$$

where 'e' denotes the elemental division, $\mathbf{q}_e$ and $\ddot{\mathbf{q}}_e$ are vectors of nodal displacements and accelerations, respectively. $\mathbf{M}_e$ and $\mathbf{K}_e$ are, respectively, mass and stiffness matrices that can be computed by integrating over the element area A and using the known inertia matrix $\mathbf{I}$ and the strain–displacement $\mathbf{B}$ and elasticity $\mathbf{E}$ matrices of the element as follows:

$$\mathbf{M}_e = \int_A \mathbf{N}^T \mathbf{I} \mathbf{N} \, \mathrm{d}A \quad \text{and} \tag{15}$$

$$\mathbf{K}_e = \int_A \mathbf{B}^T \mathbf{D} \mathbf{B} \, \mathrm{d}A \tag{16}$$

As known, the formulation of the mass matrix (15) requires knowledge of the geometrical properties of the plate and the density of its material. To define the stiffness matrix (16), the strain–displacement relation (kinematic assumptions) and the strain–stress relationship (constitutive equations) of the linear dynamic behavior of plates must be known. The strains are assumed to be small so that linear strain–displacement relations are adequate. Thereby, the strains associated with the displacement field (3) in each ith layer can be expressed in term of the nodal unknowns in the form:

$$\epsilon = \mathbf{B} \mathbf{q}_e, \tag{17}$$

The stress–strain relationships based on the assumptions of orthotopic layered material (ith layer) having any fiber orientation with respect to the global coordinate system xOy (see Fig. 1) can be expressed by Hooke's law as the following:

$$\sigma = \mathbf{D} \epsilon \tag{18}$$

Here, the stress vector σ consists of the stress resultants, which are calculated by integrating the appropriate stress tensor components over the plate thickness h. The elasticity matrix $\mathbf{D}$ is, in fact, a block matrix, sub-matrices of which define the relations between the stress resultants and strains combined into different vectors depending on their mechanical meaning. For instance, assuming that the strain vector ϵ includes in-plane strains $\{\varepsilon\}$, transverse shear strains $\{\gamma\}$ and curvatures $\{\kappa\}$, the corresponding stress resultants such that membrane $\{N\}$ and transverse shear $\{Q\}$ forces and bending moments $\{M\}$, respectively, can be related as the following:

$$\begin{Bmatrix} \{N\} \\ \{M\} \\ \{Q\} \end{Bmatrix} = \begin{bmatrix} [\mathcal{A}] & [\mathcal{B}] & \mathbf{0} \\ [\mathcal{B}]^T & [\mathcal{D}] & \mathbf{0} \\ \mathbf{0} & \mathbf{0} & [\mathcal{H}] \end{bmatrix} \begin{Bmatrix} \{\varepsilon\} \\ \{\kappa\} \\ \{\gamma\} \end{Bmatrix} \tag{19}$$

It should be noted that $\mathcal{A}_{ij}$, $\mathcal{B}_{ij}$, $\mathcal{D}_{ij}$ and $\mathcal{H}_{ij}$ are extensional, bending, bending-extensional coupling and transverse shear stiffness matrix terms, respectively. The detailed definition of each matrix can be found in the literature, e.g. [23].

By assembling the element mass and element stiffness matrices, transformed into the global coordinate system, the finite element equations of motion, representing free vibrations of the plate without damping, can be expressed as

$$\mathbf{M}\ddot{\mathbf{q}} + \mathbf{K}\mathbf{q} = \mathbf{0}, \tag{20}$$

where $\mathbf{M}$ and $\mathbf{K}$ are the global mass and stiffness matrices of the plate, $\mathbf{q}$ and $\ddot{\mathbf{q}}$ are the global nodal displacement and acceleration vectors, respectively. Moreover, prescribed boundary conditions can be additionally defined as in (20).

3.2. The eigenvalue problem

To determine natural frequencies and associated normal modes of a plate, the solution of the system (20), which is referred to as the linear eigenvalue problem [16] is required. Assuming that $\mathbf{q}$ can be presented in the form:

$$\mathbf{q} = \mathbf{\Phi} \exp(\mathrm{i}\omega t) \quad \text{or} \quad \mathbf{q} = \mathbf{\Phi}(\cos(\omega t) + \mathrm{i}\sin(\omega t)), \tag{21}$$

where $\mathbf{\Phi}$ is an eigenvector or normal mode, then after introducing (21) into (20) the free vibration analysis is reduced to the standard eigenvalue extraction problem:

$$(\mathbf{K} - \lambda \mathbf{M})\mathbf{\Phi} = \mathbf{0} \tag{22}$$

Here $\lambda = \omega^2$ is an eigenvalue. This set of equations has a non-trivial solution only if the dynamic matrix $(\mathbf{K} - \lambda\mathbf{M})$ is singular. It can be shown that this takes place for a finite number of ω_i^2 depending on the order n of the dynamic matrix. The discrete set of values ω_i^2 or $f_i = \omega_i/2\pi$, $i = 1, \ldots, n$ are called natural frequencies. Each frequency corresponds to a vector $\vec{\phi}_i$, called the eigenvector, which is the solution of the system of equations:

$$(\mathbf{K} - \omega_i^2\mathbf{M})\vec{\phi}_i = \mathbf{0}, \quad i = 1, \ldots, n \tag{23}$$

The natural frequencies f_i and vectors $\vec{\phi}_i$ define a free vibration mode of a structure. In the case of absence of damping and physical or geometrical nonlinearity, the structure will vibrate indefinitely at modal frequency f_i and with mode shape $\vec{\phi}_i$. Note that the eigenvectors $\vec{\phi}_i$ are usually scaled by a multiplier.

4. Discussion of finite element models used for the calculations

The free vibration analysis of plates based on different plate theories is carried out by applying the displacement-based FEM within the ABAQUS™ [63] code. Appropriate finite element models have been developed for homogeneous isotropic and anisotropic and composite laminated and sandwich plates. The equivalent single-layer and layer-wise theories within the framework of both the CPT and FSDT formulations as well as the three-dimensional approach are embedded into those models. Natural frequencies computed by these models are compared between themselves and with the known results. A more detailed description of each FE model developed will be given later. Before this, it should be noted that for all the FE models the following simplifying assumptions are made:

- linear modal analysis is considered;
- laminated plates are made up of layers of equal thickness and the same material, and the layers are perfectly bonded together;
- sandwich plates are modelled as three-layer plates, where average material properties of different kinds of cores are used.

All the FE models were created using the pre-processor ABAQUS/CAE and only in some rare cases was the input file manually modified. The eigenvalue problem (22) for finding natural frequencies and mode shapes was solved by means of the ABAQUS/Standard solver, where either subspace iterations or the Lanczos method is implemented. A mesh of each FE model was accepted as suitable for calculations on the basis that a desired accuracy for the results at a reasonable computational effort using an Intel® Core™ 2 T5200 CPU processor (1.60 GHz) could be reached, and there were only insignificant differences between the calculated values of natural frequencies after the mesh refinement. Such mesh-sensitivity analysis of the FE models was carried out in preliminary studies. Some of the convergence studies will be shown in the paper, but a wide discussion of the convergence of finite element solutions is behind the aims of this paper.

4.1. Models based on conventional shell elements

For the finite element analysis of three-dimensional structures in which one of the dimensions – thickness is much smaller than the other two dimensions is commonly employed plate/shell finite elements. These elements can be subdivided into two distinct groups: conventional shell elements and continuum-based shell elements (continuum shell elements), which are derived from a three-dimensional solid element via appropriate kinematic constraints imposed on the displacement field.

Conventional shell elements discretize a shell-like structure by defining the nodal geometry at reference surface and have displacement and rotational degrees of freedom. The thickness and material properties of such elements are defined through their cross-section properties. In this respect, the option `GENERAL` is used to define the total characteristics of a homogeneous structure, whereas the option `COMPOSITE` can be activated to specify thickness, orientation and material for each layer of a structure with a given lay-up. ABAQUS/Standard library of conventional shell elements uses linear (first-order) or quadratic (second-order) interpolation polynomials and allows in accordance with the FSDT or neglects due to the CPT transverse shear flexibility. To avoid shear locking, typically arising when the element thickness goes to zero a reduced (low-order) integration technique is used to form the stiffness matrix of such elements. The finite elements with reduced integration are denoted by the letter `R` in their label in what follows. Additionally, first-order elements with reduced integration are supplemented by an hourglass control for stabilizing solutions [63]. Three different types of conventional shell elements, distinguished by their applicability to 'thin' and 'thick' plate/shell problems, are used in the paper for simulations:

- S8R5/S9R5 are isoparametric thin quadrilateral shell elements using quadratic element shape forms. They represent the assumptions of the CPT that can usually be applied in cases, where transverse shear flexibility is negligible and the Kirchhoff constraint must be satisfied accurately. Herewith, the Kirchhoff constraints are imposed either analytically or numerically, where the transverse shear stiffness acts as a penalty;
- S8R is a second-order iso-parametric eight-node quadrilateral thick shell element endowed by the functionalities of the FSDT. The element is required in cases when the transverse shear deformations would be taken into account in the thick shell/plate problem;

- S4/S4R are general-purpose linear quadrilateral shell elements. They can provide solutions for both 'thick' and 'thin' plate/shell problems, i.e. the thick shell theory is used as the shell thickness increases and becomes defined as a Kirchhoff thin shell elements as the thickness decreases. The S4 element's membrane response is treated with an assumed strain formulation that gives accurate solutions to in-plane bending problems, is not sensitive to element distortion, and avoids parasitic locking, while the element S4R is enhanced by hourglassing control.

Therefore, in our calculations, thin homogeneous and composite plates are modelled with the eight-node 40-DOF quadrilateral reduced integrated shell elements, S8R5, which typify the use of the CPT. The eight-node 48-DOF quadrilateral reduced integrated shell elements S8R are applied for thick plates and FE models composed of these elements correspond to using the FSDT. The four-node 24-DOF quadrilateral fully or reduced integrated linear elements, S4 or S4R are also adopted for calculations and they can be used in those both cases mainly for checking results. It is important to notice that in the shell elements relying on the FSDT, the shear flexibility is estimated by matching the shear response for the case of the shell bending about one axis, using a parabolic variation of transverse shear stress through the shell thickness based on the 3-D elasticity theory. Moreover, for modelling multilayered plates with all types of conventional shell elements, the equivalent single-layer concept is used. According to this a plate cross-section, presented by stacking layers of different properties, is treated as a statically equivalent homogeneous material. Thereby, in-plane and transverse displacement components of such plate models will be assumed equal through the entire laminate thickness.

4.2. Models based on continuum shell elements

Unlike conventional shell elements, continuum shell elements resemble three-dimensional solid elements, which have only displacement degrees of freedom. Thereby, the total number of unknowns of this shell element is identical to that of the solid element as well as the element thickness similar to the solid element, being defined from the nodal geometry. However the kinematic assumptions and the constitutive equations of these elements are similar to conventional shell elements given at the plate/shell reference surface. This allows one to express all the nodal unknowns of the solid element in terms of those defined at the reference surface of the shell element.

The eight-node 24-DOF quadrilateral continuum shell elements, SC8R with reduced integration and hourglass control are utilized for free vibration analysis of moderately thick homogeneous and composite laminated and sandwich plates. SC8R is a general-purpose first-order interpolation element incorporating both the `GENERAL` and `COMPOSITE` shell section options and including the effect of transverse shear deformation on the basis of the FSDT kinematic assumptions. Thereby, FE models elaborated with those elements will symbolize the use of the FSDT within the equivalent single-layer approach in calculations along with other FSDT finite elements mentioned earlier.

Besides, to achieve a higher resolution in the prediction of the transverse shear flexibility of composite layered plates the SC8R elements can be stacked through the plate thickness and that will mean the use of the layer-wise approach. Herewith, it is important to notice that the LWT concept implemented into the free vibration analysis of plates via a stacking sequence of continuum shell elements implies the FSDT kinematics at each layer. Typically, one element per layer across the thickness of laminates or face sheets of sandwich, and more than one element through the thickness of a sandwich core will be employed in such models.

4.3. Models based on 3D solid elements

While homogeneous and laminated composite plates are typically modelled using appropriate shell elements, some cases can require three-dimensional solid elements with one or several solid elements through the thickness. The plate models, based on 3-D finite elements, are a discrete presentation of the 3-D elasticity theory applied for plates. Of course, the use of such elements may be preferable, when transverse shear effects are predominant and the normal transverse stress cannot be ignored, as well accurate magnitudes of stresses at layer interfaces being necessary. In this respect, 3-D solid elements allow the application of a fully three-dimensional material law for plate/shell-like structures. Thus, the transverse shear stiffness as well as transverse shear stresses in this case will be calculated directly from the equilibrium equations of the stress tensor components. This provides a real distribution through the thickness of transverse shear stresses and, in turn, real behavior of plates/shells.

The linear eight-node 20-DOF first-order and the quadratic twenty-node 60-DOF second-order 3-D hexahedral (brick) elements, marked as C3D8 and C3D20, respectively, are utilized for performing the free vibration analysis of plates. The elements are optionally supplemented by the reduced-integration technique and the incompatible mode (assumed strain) assumptions. In the latter case, the letter 'I' appears in the element label. Besides, to ensure stability and accuracy of calculations with 3-D elements, techniques eliminating shear- and volumetric-locking and hourglass modes are implemented into the formulations of the elements. Additionally, it is worth noting that to reach a desirable accuracy in calculation with 3-D elements, it is necessary to monitor the element aspect ratio, which should be retained as close as possible to a regular cubic form. As a result, the number of 3-D elements used through the thickness will increase with decreasing the element in-plane dimensions. Moreover, the number of elements in the thickness direction plays a critical role for solution accuracy in thick plates and sandwich plates with a thick core. In the numerical examples presented below more than one through-the-thickness layer of the solid elements will be employed for modelling.

However, in the case of composite sandwich plates with thin face sheets a rather fine mesh of 3-D elements is required that leads to a considerable or even prohibitively expensive computational efforts. As an alleviation of this issue, FE models combining shell elements endowed by either CPT or FSDT assumptions for representing the upper and lower face sheets and 3-D solid elements for discretizing the core of sandwich plates are utilized also. These 'mixed' models embody the HSAPT for sandwich plates. In doing so, the conventional shell elements are joined to solid ones through the shell-to-solid coupling constraints that couple displacement and rotation of each shell node to average displacement and rotation of the solid surface in the vicinity of the shell node [63], while the continuum elements can be directly coupled with adjacent solid elements.

5. Numerical results and discussion

In order to evaluate the effectiveness of different types of finite element models for free vibration analysis, homogeneous isotropic and anisotropic plates, composite laminated plates with arbitrary lay-ups, and stiff- and soft-cored sandwich plates are examined herein. The numerical examples considered in the paper are chosen in correspondence with the existing analytical and numerical solutions that are available in the literature. This allows a comparison to be made between results obtained by the FEM and other methods for the same plates. The numerical results obtained and validated in this way could be considered as benchmark solutions in what follows for isotropic and anisotropic homogeneous plates, composite laminated and sandwich plates.

5.1. Isotropic plates

Firstly, isotropic square plates with all edges simply supported or clamped having length-to-thickness aspect ratios a/h of 100 and 5 corresponding to 'thin' and 'thick' plate problems, respectively, are analyzed. The material of the plates has Young's modulus of 206.8 GPa, Poisson coefficient of 0.3 and mass density of 7827 kg/m^3. The convergence study for the different mesh sizes for the simply supported and clamped thin plates is presented in Fig. 2a and b, respectively. The

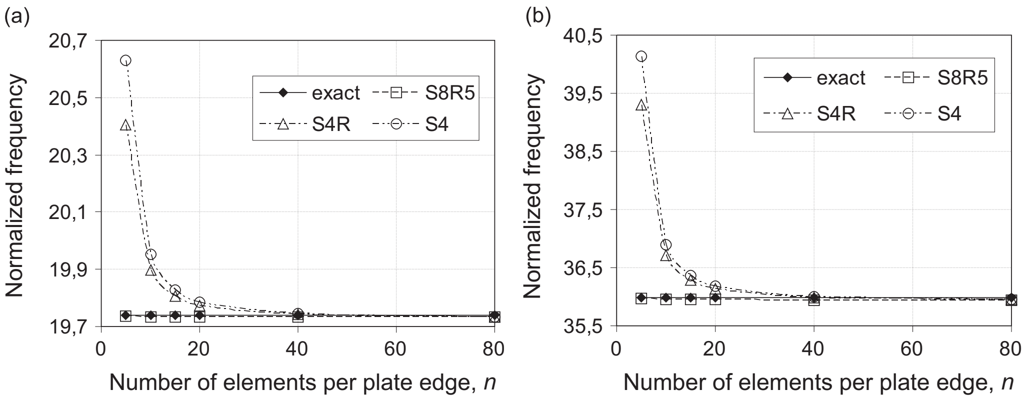

Fig. 2. Convergence of finite element solutions for the normalized fundamental frequency for the thin plate: (a) with simply supported edges; and (b) with clamped edges.

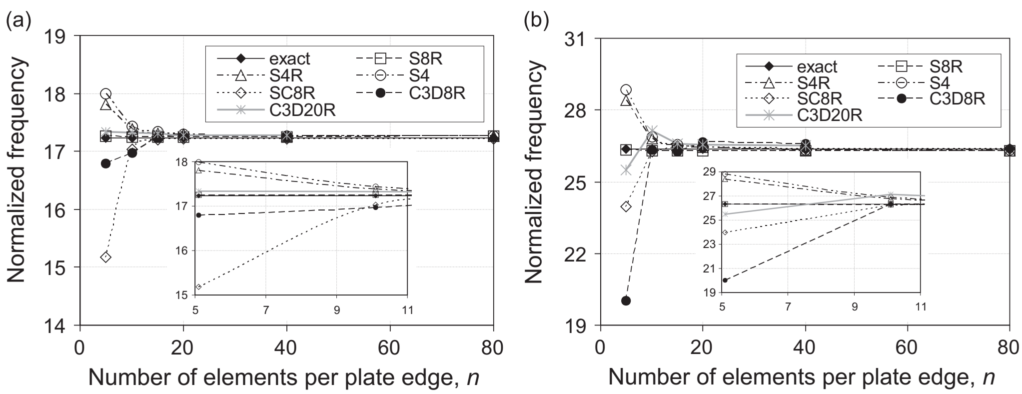

Fig. 3. Convergence of finite element solutions for the normalized fundamental frequency for the thick plate: (a) with simply supported edges; and (b) with clamped edges.

fundamental frequency, calculated with different finite elements, is validated by the exact solution for a simply supported plate, whereas the solution of the Rayleigh–Ritz method based on the beam functions in [65] is used for assessment of the fundamental frequency of the clamped plate. One can see an excellent convergence of all the elements used for the free vibration analysis with increasing mesh divisions of the plate, i.e. a number of elements n per the plate edge. The second-order element S8R5 implementing the CPT gives the most accurate solution even with the coarse mesh at both the types of boundary conditions, whereas the solutions with the first-order general purpose elements S4(R) tend toward the exact one only with increasing mesh density, but quickly enough. Herewith, the convergence rate with these elements for the clamped plate is a bit slower than for the simply supported one. To acquire the frequencies with an acceptable accuracy, a mesh with $n=10$ is needed for almost all those cases. The maximum discrepancy between the results obtained using the mesh 10×10 and the test results is less than 2.5 percent.

The convergence analysis of the FE solutions obtained for the isotropic thick plates with simply supported and clamped boundary conditions is shown in Fig. 3a and b, respectively. The numerical results for the simply supported plate are compared with the exact 3-D solution in [31], whereas the frequencies of the clamped plate are tested with respect to the 3-D solution based on Chebyshev polynomials within the Ritz method in [33]. It is should be noted that in the case of the 3-D elements, the plate was meshed in such a way that the length-to-thickness element aspect ratio was as close as possible to 1:1. As seen, all finite elements are accurate enough to predict the fundamental frequency. Herewith, the second-order shell

Table 1
Dimensionless frequencies $\overline{\omega}=\omega a^2\sqrt{\rho h/D}$ of the simply supported square isotropic plate.

a/h	Source		Mode				
			(1,1)	(1,2)	(2,1)	(2,2)	(1,3)
100	Leissa [65]		19.739	49.348	49.348	78.957	98.696
	Bhat [66]		19.739	49.348	49.348	78.957	99.304
	Liew et al. [67]		19.740	49.350	49.350	79.030	99.250
	Present, CPT	S8R5	19.734	49.323	49.323	78.869	98.644
		S4R	19.899	51.121	51.121	81.531	108.61
		S4	19.951	51.337	51.337	82.424	109.12
5	Srinivas et al. [31]		17.328	38.483	38.483	55.790	–
	Zhou et al. [33]		17.329	38.483	38.483	55.787	65.996
	Wu et al. [68]		17.148	38.267	38.133	55.185	64.204
	Shufrin et al. [69]		17.452	38.189	38.189	55.254	65.313
	Present	FSDT (S8R)	17.449	38.158	38.158	55.156	65.201
		FSDT (S4R)	17.571	39.161	39.161	56.288	67.079
		FSDT (S4)	17.609	39.274	39.274	56.645	65.928
		LWT (SC8R)	17.221	37.876	37.876	54.092	66.587
		3-D (C3D20R)	17.327	38.493	38.493	55.796	66.060

$D=Eh^3/12(1-\nu^2)$.

Table 2
Dimensionless frequencies $\overline{\omega}=\omega a^2\sqrt{\rho h/D}$ of the clamped square isotropic plate.

a/h	Source		Mode				
			(1,1)	(1,2)	(2,1)	(2,2)	(1,3)
100	Leissa [65]		35.992	73.413	73.413	108.27	131.64
	Bhat [66]		35.986	73.395	73.395	108.22	131.78
	Liew et al. [67]		35.990	73.410	73.410	108.26	131.66
	Present, CPT	S8R5	35.955	73.302	73.302	107.96	131.44
		S4R	36.714	78.027	78.027	114.08	151.72
		S4	36.898	78.554	78.554	115.98	152.76
5	Zhou et al. [33]		26.886	47.074	47.074	61.904	72.253
	Liew et al. [32]		26.932	47.139	47.139	61.936	72.299
	Wu et al. [68]		26.320	46.032	46.032	61.475	70.605
	Shufrin et al. [69]		26.817	47.128	47.128	63.504	73.112
	Present	FSDT (S8R)	26.525	46.307	46.307	62.177	70.904
		FSDT (S4R)	26.888	47.802	47.802	63.736	75.340
		FSDT (S4)	26.957	47.937	47.937	64.099	74.755
		LWT (SC8R)	26.514	46.420	46.420	62.900	72.048
		3-D (C3D20R)	26.998	47.284	47.284	63.575	72.624

$D=Eh^3/12(1-\nu^2)$.

element S8R with the FSDT and the second-order 3-D element C3D20(R) are the most accurate among them. However, the latter is the most computationally expensive because of a high density mesh required to ensure the element aspect ratio requirement. The optimal meshes for those elements can be considered as 20×20 and $10 \times 10 \times 2$, respectively. The first-order 3-D element C3D8(R) converges to the accurate solution quickly only with the activated incompatible mode, otherwise its convergence is rather slow. In this case, the continuum shell element SC8R with the mesh $20 \times 20 \times 4$ may be more preferable for calculations. One can notice again that the convergence rate for the plate with simply supported edges is faster than that for the plate with clamped sides.

Further, the first five non-dimensional frequencies of both the thin and thick isotropic square plates with simply supported and clamped boundary conditions are presented in Tables 1 and 2. The results are compared with analytical and numerical solutions available in the literature. One can see that the predicted natural frequencies of these thin plates agree very well with those in [65], where the existing well-known exact solution is presented for the plate having simply supported edges and the Ritz method is used to calculate the frequencies of the clamped plate. Also, the results are found to be in very good agreement with solutions obtained by using the Rayleigh–Ritz method employing a set of beam characteristic orthogonal polynomials in [66] and with plate orthogonal functions in [67]. For the thick plates, one can clearly see that the calculated frequencies are in good accordance with solutions in [68], where the differential cubature method with the FSDT assumptions has been utilized, and results obtained by the Kantorovich solution procedure within the HSDT assumptions in [69]. Moreover, they are close to the 3-D solutions presented in [31] for simply supported edges and in [32,33] for clamped edges of the thick plate.

Analyzing the results obtained by different computational models in Tables 1 and 2 it is obvious that the CPT models presented by either the S8R5 or the S4(R) elements are accurate in the case of the thin plates only. Herewith, the accuracy of the second-order shell element is higher than that of the linear shell elements at the same mesh. While, either FSDT models developed with the elements S8R and SC8R or 3-D models exploiting the solid elements C3D20(R) have to be used to provide accurate results for the thick plates, when the transverse shear flexibility and second-order interpolation are desired. One needs to note that the 3-D FE models demand a more refined mesh with 3795 DOF against 600 DOF for the second-order conventional shell elements and this may make the predictions with 3-D elements computationally very expensive in practical applications.

5.2. Orthotropic plates

The free vibration analysis of orthotropic homogeneous plates has been performed for the cases when the principal orthotropic directions can coincide or not coincide with the reference coordinate system of the plate. Both thin and thick orthotropic plates are examined. At the beginning, a square orthotropic thin plate with completely free edges is considered. The material properties having the principal orthotropic directions coinciding with the global coordinate system and geometrical dimensions of the plate are listed in Table 3. The FE models are developed using the CPT assumptions implemented into both the second-order thin shell element S8R5 and the first-order general-purpose shell elements S4(R). The convergence analysis similar to that in the previous Section is carried out too. The convergence rate of the finite element

Table 3
Dimensions and material properties of the orthotropic thin plate.

$a=b$ (m)	h (m)	E_1 (MPa)	E_2 (MPa)	$G_{12}=G_{13}=G_{23}$ (MPa)	ρ (kg/m^3)	ν
0.254	1.483×10^{-3}	1.297×10^5	1.027×10^4	7.312×10^3	1584	0.33

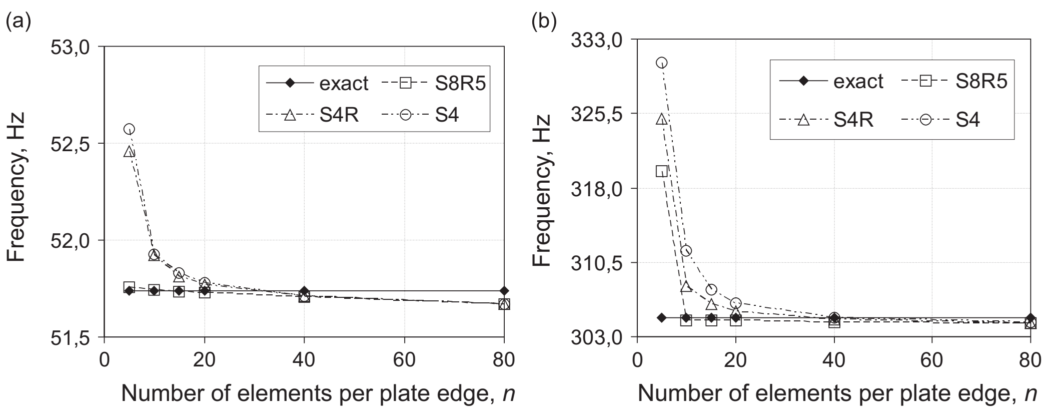

Fig. 4. Convergence of finite element solutions of the thin orthotropic plate: (a) the lowest frequency; and (b) the eighth frequency.

solutions obtained with three types of elements for the lowest and eighth natural frequencies depending of the number of elements per plate edge is shown in Fig. 4. It is seen that the discrepancy between the numerical results for all the elements used on the mesh 20×20 and the 3-D exact solutions presented in [70] does not exceed 0.5 percent for both the frequencies.

In Table 4 the first eight natural frequencies calculated with the FE models with S8R5 and S4(R) elements based on the CPT are compared with results obtained by using the 3-D exact solutions in terms of Fourier series in [70] and utilizing the superposition method in [71]. One can see an excellent agreement between the frequencies, where the largest discrepancy is about 1 percent for the higher modes. Thereby, the finite element models based on the CPT are well suited for modelling free vibrations of thin orthotropic plates in the case, when the principal orthotropic directions coincide with the reference axes of the plate.

In the next example the model based on the CPT is applied for the free vibration analysis of orthotropic thin ($a/h=100$) plates with two different boundary conditions and four angles of material orthotropy. The material properties of orthotropic plates are accepted as such that satisfy the following equalities: $E_1=5E_2$ and $G_{12}=E_1(1-\nu_{12})/2(5-\nu_{12}\nu_{21})$. In simulations we assigned $E_2=5000$ MPa, $\nu_{12}=\nu_{21}=0.3$ and $\rho=1584$ kg/m^3. Table 5 presents the first five dimensionless frequencies of the plate with two simply supported opposite edges and the other two clamped edges (CSCS) and the plate with fully clamped edges (CCCC). Here, the notations ‘S’ and ‘C’ mean clamped and simply supported fixations of the edges, respectively. From Table 5 it is obvious that the calculated frequencies agree very well with those obtained by using Green functions for solving the governing equations of motion in [72]. The mode shapes associated with the natural frequencies computed for the clamped orthotropic thin plate are shown in Fig. 5.

Next the natural frequencies of a thick ($a/h=10$) orthotropic square plate with simply supported edges are calculated. The material properties of the orthotropic plate taken are the same as in [31] and are listed in Table 6. The simulations are performed with FSDT finite element models, developed with the conventional general-purpose S4R and special thick S8R and continuum SC8R shell elements, and 3-D models incorporating solid linear C3D8(R,I) and quadratic C3D20R elements. The normalized frequencies computed by using those FE models and obtained by applying the 3-D elasticity equations in [31] and the third-order shear deformation theory in [75] are compared in Table 7. The percentage relative errors between the computational FSDT and 3-D models and the exact 3-D solution in [31] for the first 13 frequencies are shown in Fig. 6. The diagram indicates that the 3-D finite element model with quadratic solid elements provides much better results than

Table 4
Natural frequencies (Hz) of the thin orthotropic plate with completely free boundary.

Mode no	Hurlebaus et al. [70]	Gorman [71]	Present, CPT	
			S8R5	S4R
1	51.76	51.74	51.728	51.769
2	60.17	60.17	60.173	60.399
3	121.4	121.4	121.29	121.74
4	165.9	165.9	165.86	168.21
5	212.6	212.6	212.53	213.33
6	228.6	228.5	228.43	230.90
7	236.6	236.5	236.39	237.09
8	304.9	304.8	304.60	305.51

Table 5
Dimensionless frequencies $\varpi=\omega a^2\sqrt{\rho h/D}$ of the thin orthotropic square plate.

BCs	Mode no	0°		15°		30°		45°	
		CPT[a]	[72][b]	CPT[a]	[72][b]	CPT[a]	[72][b]	CPT[a]	[72][b]
CSCS	1	53.129	53.060	51.613	51.571	47.734	47.707	42.843	42.823
	2	70.667	70.481	71.857	71.752	74.333	74.256	76.486	76.387
	3	111.68	110.24	114.67	114.10	119.98	119.68	103.69	103.43
	4	140.43	139.41	134.56	134.18	120.71	120.19	123.64	123.28
	5	154.41	153.30	152.91	152.46	151.17	150.78	155.52	154.96
CSCS	1	57.266	57.145	56.043	55.998	53.656	53.618	52.506	52.470
	2	85.889	86.030	87.157	86.958	1.144	90.926	94.899	94.635
	3	139.18	137.15	136.92	136.54	124.26	123.94	116.12	115.86
	4	142.47	142.57	140.83	139.86	143.56	143.12	144.29	143.91
	5	163.05	160.71	163.13	162.38	169.31	167.90	183.11	181.17

$D=E_1h^3/12(1-\nu_{12}\nu_{21})$.
[a] Present results.
[b] Results of Whitney and Pagano.

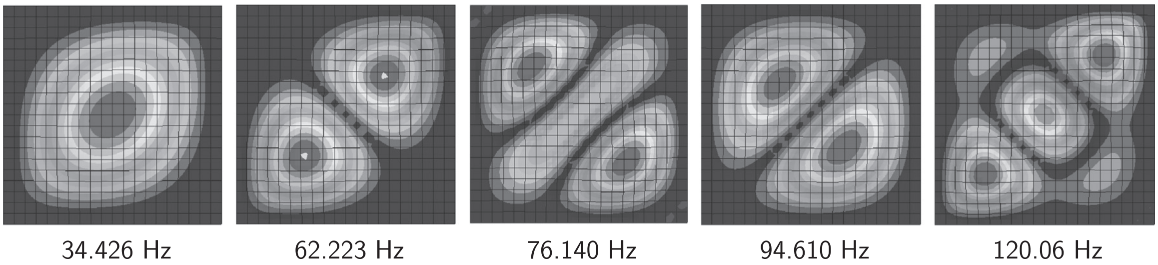

Fig. 5. The first five mode shapes of the clamped orthotropic thin square plate with angle of material orthotropy of 45°.

Table 6
Dimensions and material properties of the orthotropic thick plate.

$D_{1111}\times10^4$ (MPa)	$D_{1122}\times10^4$ (MPa)	$D_{1133}\times10^4$ (MPa)	$D_{2222}\times10^4$ (MPa)	$D_{2233}\times10^4$ (MPa)	$D_{3333}\times10^4$ (MPa)	$D_{1212}\times10^4$ (MPa)	$D_{1313}\times10^4$ (MPa)	$D_{2323}\times10^4$ (MPa)	ρ (kg/m^3)	ν
16.0	3.73	0.172	8.69	1.57	8.48	0.421	2.56	4.27	7827	0.3

Table 7
Dimensionless frequencies $\overline{\omega}=\omega h\sqrt{\rho/C_{11}}$ of the simply supported thick orthotropic square plate.

Mode	Present						[31][a]	[75][b]
	FSDT		LWT	3-D				
	(S4R	S8R)	SC8R	(C3D8R	C3D8I	C3D20R)		
(1,1)	0.0474	0.0475	0.0473	0.0468	0.0474	0.0470	0.0474	0.0474
(1,2)	0.1032	0.1039	0.1031	0.1021	0.1033	0.1023	0.1033	0.1031
(2,1)	0.1187	0.1197	0.1180	0.1177	0.1188	0.1168	0.1188	0.1197
(2,2)	0.1692	0.1703	0.1677	0.1670	0.1694	0.1669	0.1694	0.1694
(1,3)	0.1884	0.1921	0.1898	0.1869	0.1888	0.1885	0.1888	0.1897
(3,1)	0.2178	0.2217	0.2169	0.2161	0.2181	0.2137	0.2180	0.2218
(2,3)	0.2469	0.2501	0.2458	0.2437	0.2476	0.2437	0.2475	0.2460
(3,2)	0.2619	0.2653	0.2594	0.2588	0.2625	0.2564	0.2624	0.2638
(1,4)	0.2959	0.3065	0.3019	0.2934	0.2969	0.2930	0.2969	0.2963
(3,3)	0.3310	0.3352	0.3275	0.3264	0.3319	0.3233	0.3319	0.3298
(4,1)	0.3311	0.3411	0.3316	0.3286	0.3320	0.3266	0.3320	0.3388
(2,4)	0.3463	0.3552	0.3486	0.3422	0.3476	0.3401	0.3476	0.3442
(4,2)	0.3696	0.3782	0.3677	0.3656	0.3707	0.3650	0.3707	0.3746

$C_{11}=160$(GPa).
[a] Results of Srinivas et al.
[b] Results of Kant and Swaminathan.

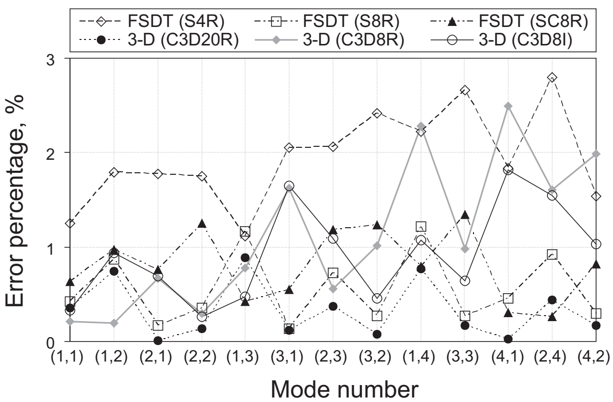

Fig. 6. Comparison of the accuracy of the different computational finite elements used for the free vibration analysis of the thick orthotropic plate.

Table 8
Material properties of the laminated plate.

Materials	E_1/E_2	G_{12}/E_2	G_{23}/E_2	ν_{12}	ν_{23}	Common	ρ (kg/m^3)
E-Glass/Epoxy	2.45	0.48	0.342	0.23	0.462	$E_3=E_2$	2100
Boron/Epoxy	11	0.34	0.346	0.21	0.444	$G_{12}=G_{13}$	2030
Graphite/Epoxy	15.4	0.79	0.79	0.3	0.675	$\nu_{13}=\nu_{12}$	1627

Table 9
Dimensionless frequencies $\overline{\varpi}=\omega a^2\sqrt{\rho h/D_0}$ of the simply supported symmetrical five-layer cross-ply thin square plates.

Mode		(1,1)	(1,2)	(2,1)	(2,2)	(1,3)	(2,3)	(3,1)	(3,2)
				E-Glass/Epoxy					
Leissa et al. [9]		15.193	35.894	42.344	60.770	71.569	94.504	88.395	105.44
Chao et al. [74]		14.862	35.063	41.330	59.367	69.779	92.217	86.090	102.79
CPT[a]	S8R5	15.146	35.727	42.105	60.297	71.023	93.497	87.439	104.10
	S4R	15.174	36.013	42.496	60.746	72.592	94.903	89.548	105.96
3-D[a]	C3D8	15.089	35.545	42.407	60.135	72.833	94.030	87.435	105.14
	C3D20R	15.090	35.603	42.474	60.346	73.004	94.247	87.904	105.54
				Boron/Epoxy					
Leissa et al. [9]		11.039	24.037	36.790	44.157	49.281	63.520	81.425	86.002
Chao et al. [74]		10.778	23.445	35.793	42.172	45.698	61.724	78.343	83.170
CPT[a]	S8R5	10.986	23.843	35.984	43.272	48.418	62.103	78.938	82.892
	S4R	11.012	24.010	36.460	43.666	49.361	62.900	79.558	84.116
3-D[a]	C3D8	10.951	23.901	36.654	43.218	49.361	63.192	81.616	86.264
	C3D20R	10.976	23.936	36.709	43.371	49.555	63.738	81.789	86.643
				Graphite/Epoxy					
Leissa et al. [9]		11.290	24.034	37.085	45.159	48.362	64.470	81.205	83.230
Chao et al. [74]		10.729	22.794	35.058	42.712	45.698	60.888	76.221	78.267
CPT[a]	S8R5	11.216	23.797	36.149	44.052	47.423	62.704	80.484	82.575
	S4R	11.244	23.952	36.652	44.474	48.283	63.481	79.300	83.275
3-D[a]	C3D8	11.200	24.269	36.392	45.067	48.589	63.756	82.058	83.448
	C3D20R	11.199	24.306	36.447	45.255	48.908	64.313	81.936	83.627

$D_0=E_1h^3/12(1-\nu_{12}^2)$.
[a] Present results.

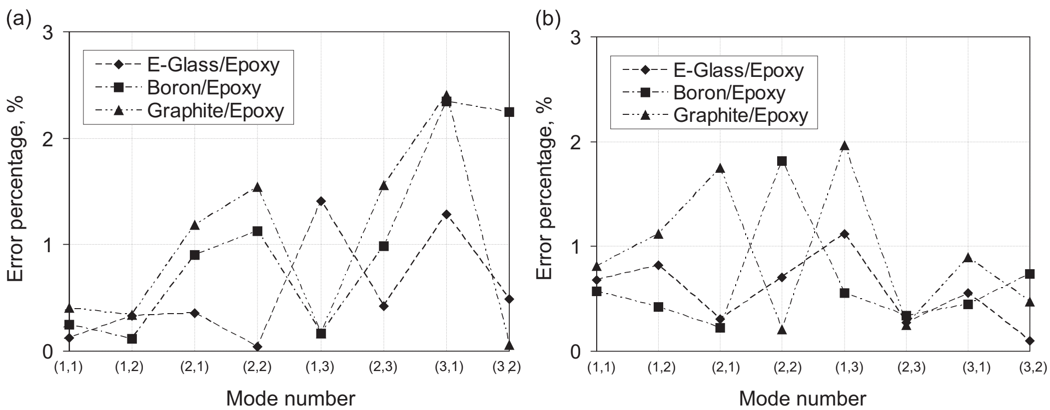

Fig. 7. A quantitative assessment of the accuracy for the natural frequencies of five layers cross-ply laminated thin plate, calculated based on (a) the model involving the CPT; and (b) the 3-D model.

other models used, but it is the most computationally expensive. At the same time, the use of the FSDT model developed with the special thick second-order shell elements and continuum shell elements gives accurate enough results, which are even comparable with the 3-D solutions resulting from the models with linear solid elements. The model developed with the general-purpose first-order shell elements gives results which are a little worse in this case, but with less computational expense.

5.3. Laminated plates

This series of examples is used to assess the accuracy of different FE models for the analysis of symmetric and antisymmetric composite laminated plates. Natural frequencies of five-layer symmetrical cross-ply and four-layer symmetrical angle-ply thin ($a/h = 50$) square plates with simply supported edges are calculated at the beginning. Three types of materials namely E-Glass/Epoxy, Boron/Epoxy and Graphite/Epoxy are considered for these plates. Properties of those materials, presented in the form of dimensionless stiffness constants are shown in Table 8. The first eight normalized natural frequencies of the cross-ply laminated plates computed using the FE models based on the CPT within ESL approach with S8R5 and S4(R) elements and the 3-D elasticity theory with C3D8(R,I) and C3D20R elements in comparison with those calculated by applying the Ritz method within the CPT in [9] and the 3-D elasticity equations in [74] are presented in Table 9. The percentage relative errors for the first eight frequencies between the computed results and the 3-D solution in [74] are presented in Fig. 7. For the CPT model the errors are larger for the higher frequencies and increase with increasing the material orthotropy ratio E_1/E_2, as seen in Fig. 7a. Thus, the CPT models are able to capture with good accuracy mainly at lower frequencies and are only accurate for materials with low orthotropy ratio. The 3-D model is less sensitive to the mode number being calculated and orthotropic material properties, Fig. 7b. Nevertheless, from the standpoint of the compromise between the accuracy and computational efforts, the CPT may prevail in the cases of thin laminates.

Table 10 shows three dimensionless natural frequencies of four-layer symmetric angle-ply thin plates computed with the CPT FE model and those obtained in papers [9] and [74]. One can see that the predicted frequencies are in good agreement

Table 10
Dimensionless frequencies $\overline{\omega} = \omega a^2\sqrt{\rho h/D_0}$ of the simply supported four-layer angle-ply thin square plates.

Source		$[0°]_S$			$[\pm 30°]_S$			$[\pm 45°]_S$		
		$\overline{\omega_1}$	$\overline{\omega_3}$	$\overline{\omega_5}$	$\overline{\omega_1}$	$\overline{\omega_3}$	$\overline{\omega_5}$	$\overline{\omega_1}$	$\overline{\omega_3}$	$\overline{\omega_5}$
E-Glass/Epoxy										
Leissa et al. [9]		14.18	38.37	57.59	15.22	40.18	66.71	15.49	40.16	71.00
Chao et al. [74]		15.19	44.42	64.53	16.02	42.62	71.68	16.29	41.63	77.56
CPT[a]	S8R5	15.02	43.98	63.84	15.75	42.02	70.57	15.99	40.92	76.37
	S4R	15.18	44.59	65.45	15.99	42.71	72.44	16.26	41.67	78.47
Boron/Epoxy										
Leissa et al. [9]		9.552	25.81	31.92	12.42	33.63	46.40	13.13	33.59	49.98
Chao et al. [74]		11.04	30.91	44.16	12.83	36.62	52.13	13.46	34.94	57.59
CPT[a]	S8R5	10.893	30.46	42.29	12.05	34.01	47.19	12.41	31.77	52.48
	S4R	11.00	31.32	43.43	12.64	35.97	50.96	13.20	34.17	56.94
Graphite/Epoxy										
Leissa et al. [9]		10.06	23.89	33.58	12.42	34.25	47.33	13.05	33.82	50.96
Chao et al. [74]		11.29	28.69	45.16	12.66	36.67	51.84	13.17	34.76	57.61
CPT[a]	S8R5	11.17	28.33	39.79	12.14	35.27	49.02	12.48	32.91	55.06
	S4R	11.26	28.96	44.75	12.45	35.95	50.47	12.88	33.76	56.57

$D_0 = E_1 h^3/12(1-\nu_{12}^2)$.
[a] Present results.

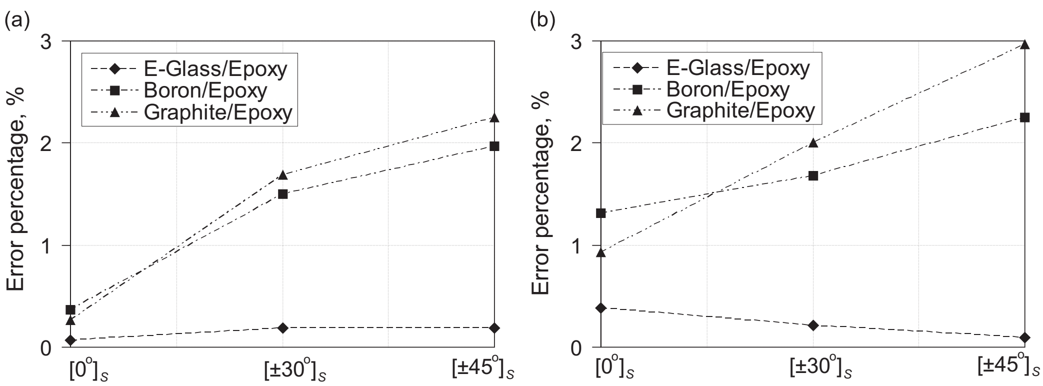

Fig. 8. A quantitative assessment of the accuracy for the natural frequencies of four layers angle-ply laminated thin plate calculated based on the CPT depending on the reinforcement angle: (a) the first frequency; and (b) the third frequency.

with the reference solutions. The percentage relative differences between the computed results and the 3-D solution in [74] for the first and third natural frequencies of the plates with different reinforcement angles in the lay-up are shown in Fig. 8.

We can identify that the accuracy of the FE model, implementing the CPT in the predictions of natural frequencies highly, depends on the angle of reinforcement. The more the reinforcement direction deviates from the reference coordinate axes, the less the prediction accuracy of the CPT model is.

In this example the fundamental frequencies of simply supported three-, five- and nine-layer symmetric cross-ply thick ($a/h=5$) square plates are calculated. The finite element models based on the FSDT within both the ESL and LWT concepts and 3-D theory of elasticity are utilized. The material properties of the plates are taken for the wide range of material anisotropy ratios E_1/E_2 from 3 to 40 and $E_2=E_3$, $G_{12}=G_{13}=0.6E_2$, $G_{23}=0.5E_2$, $\nu_{12}=\nu_{13}=\nu_{23}=0.25$. The FSDT plate models assuming the ESL are presented by conventional shell elements S4R and S8R. The LWT model with the FSDT assumptions for each layer is created by stacking through-the-thickness the continuum shell elements SC8R. Four elements per layer in three layer, two elements per layer in five layer and one element per layer in nine layer plates in the thickness direction are used in the simulations. In doing so, the plate is discretized by the FE mesh, where the element length-to-thickness aspect ratio is kept not less than 2:1. The 3-D finite element models are composed of the C3D8(R,I) and C3D20R elements of the regular cubic form. The two first-order 3-D elements, but one second-order 3-D element per layer are utilized in the tree-layer laminate and one element per layer for all other 3-D models. The exact 3-D solution in [31] and results obtained using the FSDT in [73] and the HSDT in [75] are invoked for comparison with the results calculated herein. The values of the frequencies are summarized in Table 11, and the relative differences between the FE predictions and the test 3-D solution in [31] for the five- and nine-layer laminated plates are shown in Fig. 9.

As one sees from Table 11 and Fig. 9, all the FE models can provide a correct value of the fundamental frequency within accepted engineering precision. Herewith, the 3-D models based on the second-order and the first-order with the assumed strain assumptions solid elements are the most accurate. However, they have the greatest computational cost; and this is 20 times more than for the FSDT models developed with conventional shell elements within the ESL approach. The latter models, unfortunately, have the worst accuracy among all the others. The LW model created via the stacked through-the-thickness FSDT shell elements gives results accurate enough, which are comparable with the 3-D solutions based on the linear solid elements. Thus, a compromise between the accuracy and computational efforts for modelling thick laminated plates can be gained by using the LW model.

Table 11
Dimensionless fundamental frequencies $\overline{\omega_1}=\omega_1 a^2/h\sqrt{\rho/E_2}$ of the simply supported symmetric cross-ply laminated thick square plates.

Lay-up		Source	E_1/E_2				
			3	10	20	30	40
			$[0/90^\circ/0]$				
Srinivas et al. [31]			6.6185	8.2103	9.5603	10.272	10.752
Whitney et al. [73]			6.5630	8.1847	9.2774	9.8851	10.289
Kant et al. [75]			6.5712	8.1696	9.2513	9.8595	10.269
Present	FSDT	S4R	6.5587	8.1371	9.1800	9.7460	10.112
		S8R	6.5476	8.1258	9.1700	9.7363	10.103
	LWT	SC8R	6.4927	7.9443	8.8803	9.3930	9.7325
	3-D	C3D8R	6.4926	8.0669	9.1184	9.7199	10.110
		C3D8I	6.5572	8.2113	9.3449	9.9798	10.401
		C3D20R	6.5682	8.1639	9.2381	9.8357	10.232
			$[0/90^\circ/\overline{0}]_S$				
Srinivas et al. [31]			6.6468	8.5223	9.9480	10.785	11.344
Whitney et al. [73]			6.5844	8.4201	9.8265	10.679	11.267
Kant et al. [75]			6.6033	8.4382	9.8246	10.644	11.196
Present	FSDT	S4R	6.5775	8.3626	9.6949	10.470	10.985
		S8R	6.5662	8.3503	9.6828	10.458	10.973
	LWT	SC8R	6.5266	8.1934	9.4194	10.123	10.588
	3-D	C3D8R	6.4724	8.2766	9.6328	10.427	10.957
		C3D8I	6.5926	8.4310	9.8177	10.635	11.183
		C3D20R	6.5951	8.4029	9.7488	10.533	11.058
			$[0/90^\circ/0/90^\circ/\overline{0}]_S$				
Srinivas et al. [31]			6.6600	8.6080	10.137	11.053	11.670
Whitney et al. [73]			6.5940	8.5196	10.037	10.954	11.579
Kant et al. [75]			6.6143	8.5422	10.055	10.964	11.581
Present	FSDT	S4R	6.5954	8.5001	9.9844	10.869	11.450
		S8R	6.5841	8.4874	9.9713	10.856	11.438
	LWT	SC8R	6.5371	8.3245	9.6677	10.449	10.967
	3-D	C3D8R	6.5703	8.4852	9.9852	10.885	11.494
		C3D8I	6.6071	8.5315	10.039	10.945	11.558
		C3D20R	6.6077	8.5213	10.013	10.906	11.509

The non-dimensional fundamental frequencies of simply supported antisymmetric cross-ply two-, four-, and ten-layer thin and thick square plates in comparison with those obtained using the 3-D elasticity theory in [74] and calculated with alternative FE models implementing refined transverse shear theories in [20,76] and [77] are collected in Table 12. The material properties of the individual layers for all examined laminates are the following: $E_1/E_2 = 10$ or 40, $E_2 = E_3$, $G_{12} = G_{13} = 0.6E_2$, $G_{23} = 0.5E_2$, $\nu_{12} = \nu_{13} = \nu_{23} = 0.25$. The length-to-thickness ratios of the laminates were taken as $a/h = 10$ for thick and $a/h = 100$ for thin plates. The plate models involving either the CPT and FSDT with conventional shell elements within the ESL approach or the LWT via stacked continuum shell elements or 3-D solid elements are used again. The LW and 3-D models are meshed accounting for the proper element length-to-thickness aspect ratios. Herewith, one element per layer in the 10-layer plate and two elements per layer in two- and four-layer plates are used. It can be seen from Table 12 that the calculated frequencies are in good agreement with the solutions given in the mentioned references. The percentage relative errors of the calculated fundamental frequencies for the thin and thick laminates with respect to the results in [74] are presented in Fig. 10.

As seen, the use of the CPT models leads to accurate enough results for the thin laminates, whereas the FSDT models give good enough predictions for the thick laminates. Although, the accuracy of the FSDT model based on the general-purpose S4R element that uses a simple bending kinematic and low order shape function is less satisfactory in the thick problem. The

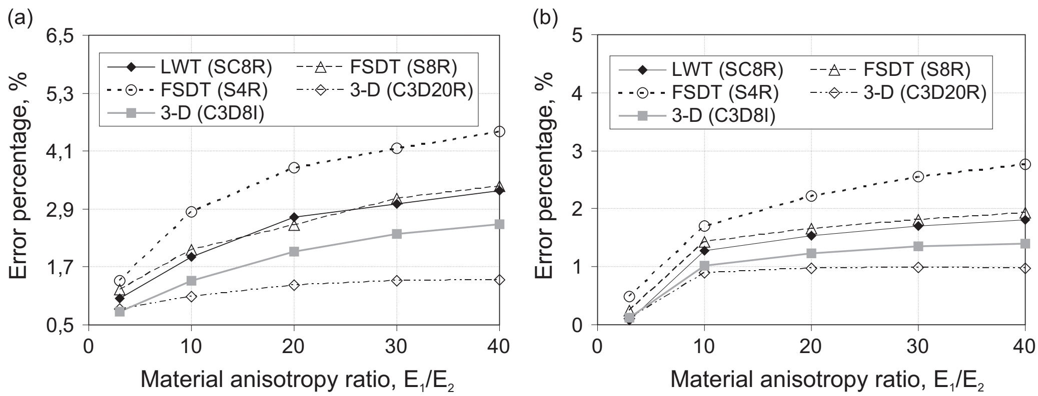

Fig. 9. A quantitative assessment of the accuracy for the fundamental frequency of the symmetric cross-ply thick laminates with (a) five layers; and (b) nine layers.

Table 12
Dimensionless fundamental frequencies $\overline{\omega_1} = \omega_1 a^2/h\sqrt{\rho/E_2}$ of the simply supported antisymmetric cross-ply laminated thin and thick plates.

E_1/E_2	Source		2 layers		4 layers		10 layers	
			$a/h = 10$	100	10	100	10	100
10	Chao et al. [74]		7.7343	8.0815	9.3888	10.011	9.8409	10.485
	Owen et al. [76]		7.8699	8.1477	9.5385	10.093	9.9648	10.574
	Argyris et al. [77]		7.7644	8.1090	9.3764	10.049	9.8664	10.529
	CPT[a]	S8R5	–	8.1304	–	10.073	–	10.554
	FSDT[a]	S4R	7.7795	8.1551	9.4214	10.094	9.9044	10.584
		S8R	7.7809	–	9.4005	–	9.8789	–
	LWT[a]	SC8R	7.7456	–	9.3783	–	9.8269	–
	3-D[a]	C3D8R	7.6267	–	9.1368	–	9.8519	–
		C3D8I	7.7809	–	9.4563	–	9.8987	–
		C3D20R	7.7877	–	9.4416	–	9.8985	–
40	Reddy et al. [20]		10.610	11.538	14.883	17.493	15.793	18.821
	Chao et al. [74]		10.313	11.258	14.478	17.226	15.656	18.521
	Owen et al. [76]		10.501	11.320	14.736	17.304	15.802	18.639
	Argyris et al. [77]		10.362	11.289	14.346	17.263	15.680	18.601
	CPT[a]	S8R5	–	11.297	–	17.273	–	18.610
	FSDT[a]	S4R	10.276	11.332	14.457	17.324	15.709	18.664
		S8R	10.263	–	14.423	–	15.673	–
	LWT[a]	SC8R	10.291	–	14.284	–	15.673	–
	3-D[a]	C3D8R	10.077	–	14.124	–	15.351	–
		C3D8I	10.408	–	14.638	–	15.727	–
		C3D20R	10.419	–	14.507	–	15.706	–

[a] Present results.

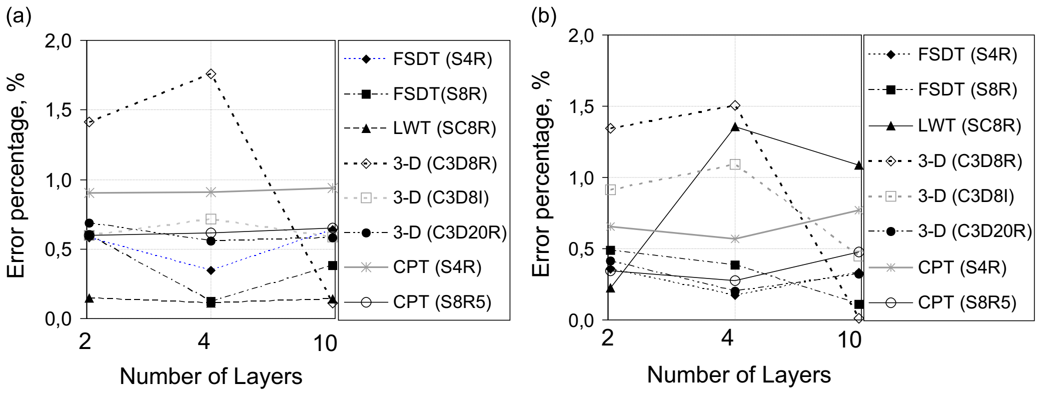

Fig. 10. A quantitative assessment of the accuracy for the fundamental frequency of the antisymmetric cross-ply laminates with (a) $E_1/E_2=10$; and (b) $E_1/E_2=40$.

Table 13
Dimensions and material properties of the simply supported rectangular sandwich plate.

Component	a (m)	b (m)	h (m)	ρ (kg/m^3)	E (GPa)	G_{13} (GPa)	G_{23} (GPa)	ν
Face sheet	1.83	1.22	4.06×10^{-4}	2770	68.9	–	–	0.33
Core			0.0064	122	–	0.134	0.052	0.32

Table 14
Natural frequencies (Hz) of the simply supported rectangular sandwich plate.

Mode no		ω_1	ω_2	ω_3	ω_4	ω_5	ω_6	ω_7	ω_8	ω_9	ω_{10}
[78][a]	'*EXP*'	23	45	69	78	92	129	133	152	169	177
	'*ANL*'	23	45	71	80	91	126	129	146	165	174
[80][b]		23.4	45.0	71.4	81.3	92.7	128.3	133.7	150.4	171	180
[81][c]		22.2	43.3	68.7	77.1	89.6	126.1	141.8	160.6	167	180
CPT[d]	S8R5	23.3	44.5	70.9	79.6	91.7	126.0	128.1	148.9	169	173
	S4R	23.7	46.2	78.8	88.2	98.9	136.6	158.3	192.6	200	208
FSDT[d]	S8R	23.2	44.5	70.3	79.8	91.0	125.5	129.1	146.2	166	174
LWT[d]	SC8R	23.6	45.5	75.0	83.5	96.4	133.4	139.8	169.8	188	190
3-D[d]	C3D20R	23.3	44.5	70.2	79.7	90.9	125.3	128.4	145.0	165	173
HSAPT[d]	S4R/C3D8R	23.1	44.1	70.4	78.2	91.1	124.6	124.6	148.4	168	170
	S8R/C3D20R	22.9	43.6	69.5	77.0	89.3	124.9	129.1	148.9	171	172
	SC8R/C3D8R	23.9	45.8	71.7	80.4	94.2	127.0	129.3	149.5	171	175

[a] Results of Raville and Veng.
[b] Results of Nayak et al.
[c] Results of Malekzadeh et al.
[d] Present results.

increase of the integration points through the thickness of the element does not improve the results. The accuracy of the 3-D models is much better, but they demand the biggest computational efforts. In this respect, the LW model can be considered as an alternative to computationally expensive 3-D models for modelling thick laminates.

5.4. Sandwich plates

Sandwich plates can be considered as a three-layer laminated plate consisting of two thin stiff layers, called face sheets, separated by a thick and weak layer, referred to as core [23]. Unlike a standard laminate, where, as usual, layers of equal thickness and the same material are composed together, sandwich constituents typically possess extremely different mechanical and geometrical properties through the thickness. The ratio of Young's moduli of the face sheets to the core typically lies between 500 and 1000 and even more. As such, the core can be very flexible relative to the face sheets. This flexibility leads to a change in the height of the core and, as a result, there exists a nonlinear cross section pattern, which the plate theories that work well for laminates fail to predict. Thereby, free vibration analysis of sandwich plates requires an appropriate approach accounting for overall modes, localized ones and through the thickness. In this respect, the HSAPT [50] has successfully been used in the analysis of the majority of actual sandwich constructions, instead of other assumptions called as an anti-plane stress state, which are mostly valid for stiffer metallic honeycomb cores.

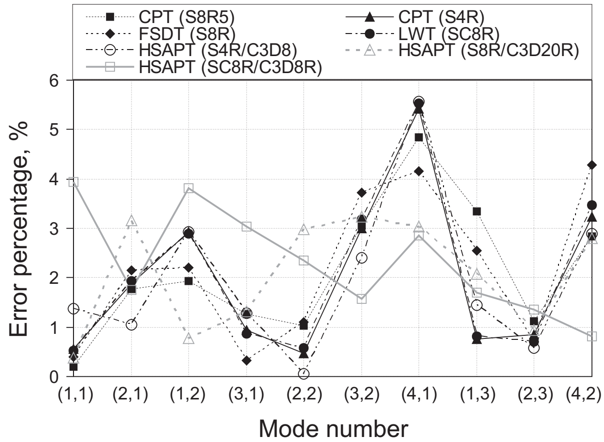

Fig. 11. Comparison of the accuracy of the different computational finite elements used for the free vibration analysis of the thin sandwich plate.

Table 15
Material properties of the simply supported thick sandwich plate.

Component	E_1 (GPa)	E_2 (GPa)	E_3 (GPa)	G_{12} (GPa)	G_{13} (GPa)	G_{23} (GPa)	ν	ρ (kg/m^3)
FRP face sheets	24.51	7.77	7.77	3.34	3.34	1.34	0.25	1800
PVC C70.130 core	0.1036	0.1036	0.1036	0.05	0.05	0.05	0.32	130

Table 16
Dimensionless frequencies $\varpi = \omega a^2 \sqrt{\rho_c / E_c}$ of simply supported sandwich square plates.

Mode no		[0/90°/0/*CORE*/0/90°/0]				[45°/−45°/45°/*C*/−45°/45°/−45°]			
		$\overline{\omega_1}$	$\overline{\omega_2}$	$\overline{\omega_3}$	$\overline{\omega_4}$	$\overline{\omega_1}$	$\overline{\omega_2}$	$\overline{\omega_3}$	$\overline{\omega_4}$
[79][a]		15.28	28.69	30.01	38.86	16.38	29.65	29.65	40.00
[81][b]		14.83	26.91	27.47	35.57	15.53	27.36	27.36	36.39
FSDT[c]	S4R	15.79	29.01	29.64	38.47	16.94	29.91	29.91	39.63
	S8R	15.77	28.88	29.51	38.33	16.92	29.79	29.79	39.51
LWT[c]	SC8R	15.01	27.10	27.63	35.70	16.31	28.54	28.54	37.63
HSAPT[c]	S4R/C3D8R	14.62	26.80	27.40	35.55	15.42	27.17	27.46	36.24
	S8R/C3D20R	14.63	26.80	27.41	35.58	15.43	27.18	27.47	36.27
	SC8R/C3D8R	14.62	26.80	27.41	35.55	15.41	27.29	27.29	36.25

[a] Results of Meunier and Shenoi.
[b] Results of Malekzadeh et al.
[c] Present results.

Free vibrations of a simply supported rectangular sandwich plate with aluminum face sheets and an aluminum honeycomb core have been studied experimentally and analytically with assumptions of an anti-plane core in [78]. The geometry and material properties of the sandwich plate are given in Table 13. In the paper the natural frequencies known from [78] are compared with those computed using appropriate FE plate models. The models embodying the CPT and FSDT are composed of the second-order thin S8R5 or first-order general-purpose S4R and second-order thick S8R conventional shell elements, respectively. In the LW model, four continuum shell SC8R elements per core and one element for each face sheet, stacked into a sequence in the thickness direction, are used. The 3-D model is presented by the second-order continuum solid elements C3D20R, where one element per face sheet and two elements per core are assigned. Finally, the HSAPT models are realized via compositions of shell and solid finite elements. Firstly the general-purpose shell elements S4R are used for the face sheets, whereas the linear 3D elements C3D8R are utilized to discretize the core. Secondly the face sheets and the core are covered by the second-order shell elements S8R and the second-order solid elements C3D20R, respectively. Thirdly, the combination of the continuum shell elements SC8R for the face sheets and the solid 3-D elements C3D8R for the core are applied. Herewith, one element per face sheet and two or more elements per core are utilized for all calculations. It should be mentioned that the HSAPT models have to attain compatibility between the shell and continuum elements. The first two models can provide it via the special shell-to-solid constraints available in the ABAQUS code, but there is no conflict between the degrees of freedom in the latter HSAPT model.

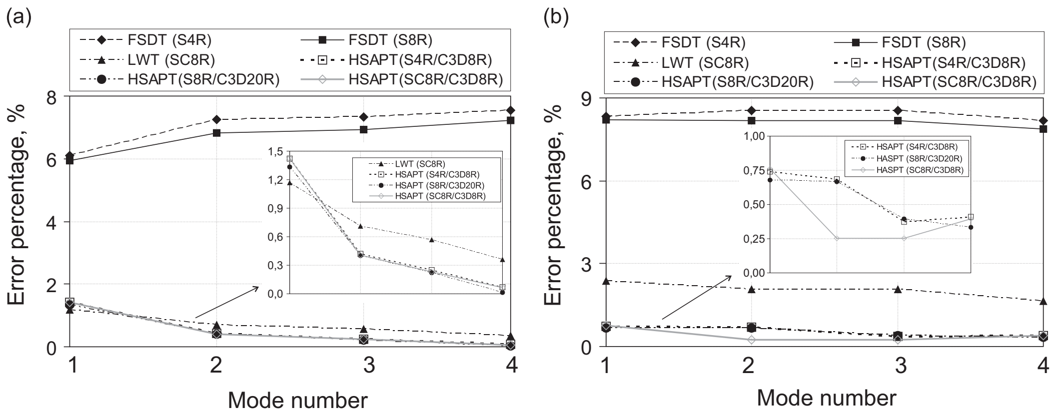

Fig. 12. Comparison of the accuracy of the finite element models used for the free vibration analysis of the thick sandwich plate: (a) with symmetric cross-ply face sheets; and (b) antisymmetric angle-ply face sheets.

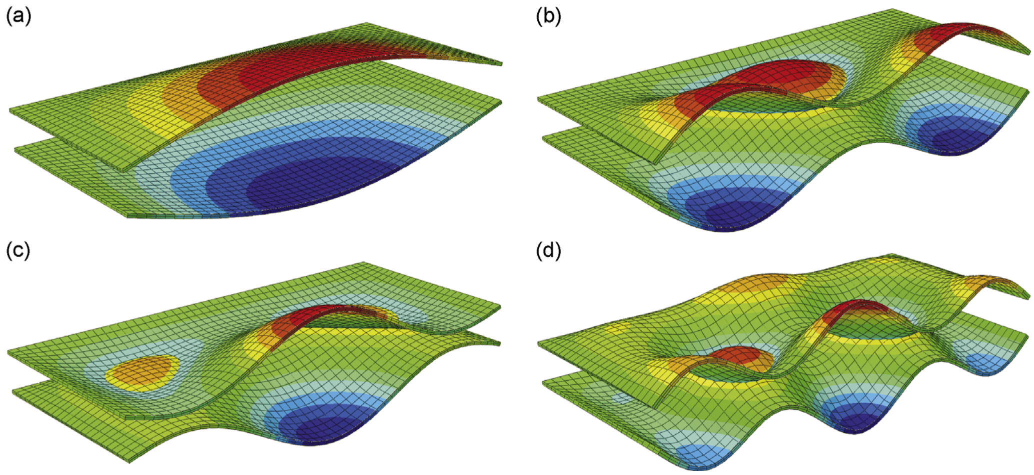

Fig. 13. Pumping (symmetric) modes in the simply supported thick sandwich plate.

The natural frequencies measured and calculated in [78] and computed in the paper for the sandwich plate are tabulated in Table 14. The relative differences between them are shown in Fig. 11. One can see that the predicted results are in close agreement with the known analytical (*ANL*) and experimental (*EXP*) frequencies as well, noting that they are in good compliance with the closed-form solutions based on the HSAPT model in [81] and the FE solutions using an assumed strain formulation of Reddy's higher-order theory in [80]. Furthermore, Table 14 and Fig. 11 show that accurate results are also provided by the FSDT models involving the conventional shell elements. Thus, these models can be adequate in the case of thin sandwich plates with a stiff core.

In the next example, the accuracy of the FE plate models of thick ($a/h = 10$) symmetric and antisymmetric square sandwich plates is evaluated by comparing the calculated frequencies with the analytical solutions based on the HSDT in [79] and results obtained with the HSAPT in [81]. The sandwich plates are composed of the laminated cross-ply or angle-ply fibre reinforced plastic (FRP) face sheets and a HEREX C70.130 polyvinyl chloride (PVC) foam core. The elastic mechanical constants corresponding to those materials, taken as in [79], are presented in Table 15. The ratio of the core thickness to the total thickness of the plate is $h_c/h = 0.88$.

Table 16 shows the first four dimensionless natural frequencies calculated in the paper and obtained by the authors in [79,81]. The same FE models, discussed above, are used for analysis of the thick sandwich plate with a soft foam core. Herewith, the models developed with solid elements are composed of four linear and two quadratic elements through the core thickness, whereas one element per face sheet is used in all the cases. As seen from Table 16, the frequencies calculated with the FSDT models and LWT model exploiting the FSDT assumptions at each layer are in good agreement with those obtained analytically using the high-order theory within the equivalent single-layered plate in the paper [79]. While the mixed shell-solid models result in the lower frequencies, compared to the results in [79], they are close to values obtained with the HSAPT assumptions in [81]. The relative differences between the finite element results and the analytical solutions in [81] are presented in Fig. 12. It is obvious that the HSAPT models enable the capture of the transverse flexibility of the core and, therefore, are more accurate for modelling sandwich plates than models based on the FSDT assumptions within both the ESL and LW concepts. The mode shapes associated with the natural frequencies of soft-cored plates may include pumping (symmetric) modes relating to the changes of the plate height. Several of such modes similar to those presented in [82] are shown in Fig. 13. It is necessary to note that the core is excluded from the figures for the sake of clearness. Thus, the mixed FE models using the solid elements for the core and shell elements for the face sheets are more preferable for modal analysis of sandwich plates.

6. Conclusions

The FEM is considered herein as one of the most effective methods allowing the handling of a variety of plate models in a unified manner. The finite element predictions of natural frequencies and appropriate mode shapes of isotropic, anisotropic, laminated and sandwich composite plates are carried out. The known plate theories are implemented into various computational models developed within the finite element package ABAQUS™ in order to evaluate the accuracy of kinematic assumptions utilized. The obtained results of the finite element studies are consistent with earlier known analytical, experimental and numerical solutions for free vibrations of selected plates. Comparisons of the results lead to the following general conclusions:

- The ideas of the CPT, which are implemented in the thin shell elements with Kirchhoff constraints S8R5(S9R5) and general-purpose shell elements S4(R), are very suitable for performing the free vibration analysis of isotropic and orthotropic thin plates. Nevertheless, it should be noticed that the latter elements are first-order and therefore they demand a finer mesh than the former ones.
- In order to analyze accurately the modal response of thick isotropic and orthotropic plates, the FE models using the FSDT assumptions within the thick second-order shell elements S8R and linear continuum shell elements SC8R can be exploited. At the same time, the models based on the general-purpose linear shell elements S4(R), which use the FSDT as a suitable option, are less accurate especially in the prediction of high frequencies of thick plates. The use of 3-D models, generated by the first- C3D8(R,I) or second-order C3D20(R) solid elements, demands a very fine mesh, and consequently has a much high computational cost than other models.
- The thin shell elements S8R5 endowed by the CPT were inadequate for prediction of the frequencies of layered plates, while they can be recommended in cases of extremely thin laminates. The slight increase of accuracy for laminated plate frequencies was gained by using the general-purpose shell element S4(R). The thick shell S8R and continuum shell SC8R elements, where the effect of transverse shear deformation is taken into account by means of the FSDT, gave satisfactory results for moderately thick and thick laminated plates. However, the obtained solutions with application of FSDT within the single-layer laminate concept in S8R and SC8R are not good when the degree of material anisotropy (E_1/E_2 ratio) increases. Comparison of the results computed in this paper with solutions known in the literature leads to the conclusion that only FE models developed with stacked through-the-thickness elements can provide more accurate results. The models of the continuum shell elements SC8R, stacked into an appropriate sequence in the thickness direction, are associated with the layer-wise approach, where the FSDT assumptions for each layer are assumed. Such models can capture more correctly variations of transverse shear deformations that yield a high enough prediction accuracy of the natural frequencies of laminated plates and allow one to attain the CPU time at a reasonable level with increased accuracy in comparison with the 3-D models. In the case of multi-layer plates, the use of 3-D models becomes numerically prohibitively expensive.
- The general approach adopted for the analysis of sandwich plates implies that they can be assumed as three-layered structures. Thereby, the FE models applied to laminates are suitable for the free vibration analysis of sandwich plates. Nevertheless, the models using only shell elements based on the FSDT have not shown a good agreement with the analytical solutions and experimental data in the case of soft cores. This is connected with the extremely different properties of the constituents composing a sandwich plate that leads to non-identical displacements in the face sheets and, as a result, a nonlinear deformed pattern through the sandwich thickness. Hence, in order to predict the frequencies of sandwich plates with greater accuracy, the application of FE models involving solid elements can be more preferable. However the latter models demand a very fine mesh and, therefore, they are often extremely computationally expensive. As an alternative to those 3-D models, the models using conventional or continuum shell elements for the face sheets and solid elements for the core can be considered. The advantages of these FE models are not so high computational cost and realistic predictions in accordance with the HSAPT.

In general, an analyst can choose a suitable finite element model depending on the requested accuracy and available numerical possibilities. However, since the FE technique is a method based on an idealization of geometry, the results will be as accurate as the idealization. Thus, mesh sensitivity needs to be considered for preliminary assessments of results. Besides, from the engineering point of view the FSDT is still an attractive approach in FE modelling due to its simplicity and low computational cost. Moreover, it is well recognized that the FSDT gives adequate solutions for global structural behavior e.g. transverse deflections, fundamental frequencies and modes, and critical buckling loads. At the same time, it is necessary to remember that this theory is inadequate for the accurate predictions of local responses such as modes and frequencies corresponding to thickness-stretch deformation (warping cross-section effect), interlaminar effects, face sheet-to-core debonding, and wrinkling phenomena of face sheets, etc. In such cases more sophisticated FE models like the models based on the LWT for laminates or the HSAPT for sandwich plates are required.

Acknowledgements

The authors would like to thank the anonymous reviewers for their valuable comments and suggestions to improve the quality of the paper. The first author acknowledgements the German Science Foundation DFG (AL 341/46-1) for supporting his research in Otto-von-Guericke University Magdeburg. The third author would like to mention that this work was also financially supported by Ministry of Science and Higher Education of Poland within the statutory research Grant no. S/20/2015.

References

[1] S. Timoshenko, S. Woinowsky-Krieger, *Theory of Plates and Shells*, Second Edition, McGraw-Hill, New York, 1961.
[2] H. Altenbach, J. Altenbach, K. Naumenko, *Ebene Flächentragwerke, Grundlagen der Modellierung und Berechnung von Scheiben und Platten*, Springer-Verlag; Berlin Heidelberg, 1998.
[3] J.N. Reddy, *Theory and Analysis of Elastic Plates and Shells*, Second Edition, CRC Press, Philadelphia, 2006.
[4] J. Altenbach, H. Altenbach, V.A. Eremeyev, On generalized Cosserat-type theories of plates and shells: *a short review and bibliography*, *Archive Applied of Mechanics* 80 (2010) 73–92.
[5] H. Altenbach, Theories for laminated and sandwich plates, *Mechanics of Composite Materials* 34 (3) (1998) 243–252.
[6] R.E. Rossi, A note on a finite element for vibrating thin orthotropic rectangular plates, *Journal of Sound and Vibration* 208 (5) (1997) 864–868.
[7] N.M. Werfalli, A.A. Karoud, Free vibration analysis of rectangular plates using Galerkin's-based finite element method, *International Journal of Mechanical Engineering* 2 (2012) 59–67.
[8] A.K. Noor, Free vibrations of multilayered composite plates, *AIAA Journal* 11 (1973) 1038–1039.
[9] A.W. Leissa, Y. Narita, Vibration studies for simply supported symmetrically laminated rectangular plates, *Composite Structures* 12 (1989) 113–132.
[10] L.X. Luccioni, S.B. Dong, Laminated composite rectangular plates, *Composites Part B* 29 (1998) 459–475.
[11] B.S. Al-Janabi, E. Hinton, D. Vuksanovich, Free vibration of Mindlin plates using finite element methods. Part I: *square plates with various edge conditions*, *Engineering Computations* 6 (1989) 90–96.
[12] M.C. Manna, Free vibration analysis of isotropic rectangular plates using a high-order triangular finite element with shear, *Journal of Sound and Vibration* 281 (2005) 235–259.
[13] J.N. Reddy, Free vibration of antisymmetric angle-ply laminated plates including transverse shear deformation by the finite element method, *Journal of Sound and Vibration* 66 (1979) 565–576.
[14] A.K. Sharma, N.D. Mittal, Free vibration analysis of laminated composite plates with elastically restrained edges using FEM, *Central European Journal of Engineering* 3 (2) (2013) 306–315.
[15] H. Altenbach, An alternative determination of transverse shear stiffnesses for sandwich and laminated plates, *International Journal of Solids and Structures* 37 (25) (2000) 3503–3520.
[16] O.C. Zienkiewich, R.L. Taylor, *The Finite Element Method*, *Fifth edition Volume 2: Solid Mechanics*, Butterworth-Heinemann, Oxford, 2000.
[17] K.J. Bathe, A. Iosilevich, D. Chapelle, An evaluation of the MITC shell elements, *Computers & Structures* 75 (1) (2000) 1–30.
[18] N.F. Hanna, A.W. Leissa, A higher order shear deformation theory for the vibration of thick plates, *Journal of Sound and Vibration* 170 (1994) 545–555.
[19] R.C. Batra, S. Aimmanee, Vibrations of thick isotropic plates with higher order shear and normal deformable plate theories, *Computers & Structures* 83 (2005) 934–955.
[20] J.N. Reddy, N.D. Phan, Stability and natural vibration of isotropic, orthotropic and laminated plates according to higher-order shear deformation theory, *Journal of Sound and Vibration* 98 (1985) 157–170.
[21] A.K. Ghosh, S.S. Dey, Free vibration of laminated composite plates—a simple finite element based on higher order theory, *Computers & Structures* 52 (3) (1994) 397–404.
[22] M.R. Aagaah, M. Mahinfalah, G.N. Jazar, Natural frequencies of laminated composite plates using third order shear deformation theory, *Composite Structures* 72 (2006) 273–279.
[23] H. Altenbach, J. Altenbach, W. Kissing, *Structural Analysis of Laminate and Sandwich Beams and Plates: An Introduction into the Mechanics of Composites*, Springer-Verlag, Berlin, 2004.
[24] H.T.Y. Yang, S. Saigal, A. Masud, R.K. Kapania, A survey of recent shell finite elements, *International Journal for Numerical Methods in Engineering* 47 (1–3) (2000) 101–127.
[25] A.K. Nayak, R.A. Shenoi, Assumed strain finite element for buckling and vibration analysis of initially stressed damped composite sandwich plates, *Journal of Sandwich Structures and Materials* 7 (2005) 307–334.
[26] S.J. Lee, H.R. Kim, FE analysis of laminated composite plates using a higher order shear deformation theory with assumed strains, *Latin American Journal of Solids and Structures* 10 (2013) 523–547.
[27] M. Karama, K.S. Afaq, S. Mistou, A new theory for laminated composite plates, *Proceedings of ImechE, Part L: Journal of Materials: Design and Applications* 223 (2009) 53–62.
[28] M. Aydogdu, A new shear deformation theory for laminated composite plates, *Composite Structures* 89 (2009) 94–101.
[29] N. Grover, B.N. Singh, D.K. Maiti, Analytical and finite element modeling of laminated composite and sandwich plates: *an assessment of a new shear deformation theory for free vibration response*, *International Journal of Mechanical Sciences* 67 (2013) 89–99.
[30] R. Kienzler, P. Schneider, Comparison of various linear plate theories in the light of a consistent second-order approximation. *Mathematics and Mechanics of Solids* 20 (7), 2015, 871-882. http://dx.doi.org/10.1177/1081286514554352.
[31] S. Srinivas, C.V. Joga Rao, A.K. Rao, An exact analysis for vibration of simply supported homogeneous and laminated thick rectangular plates, *Journal of Sound and Vibration* 12 (1970) 187–199.
[32] K.M. Liew, T.M. Teo, Three-dimensional vibration analysis of rectangular plates based on differential quadrature method, *Journal of Sound and Vibration* 220 (1999) 577–599.
[33] D. Zhou, Y.K. Cheung, F.T.K. Au, S.H. Lo, Three-dimensional vibration analysis of thick rectangular plates using Chebyshev polynomial and Ritz method, *International Journal of Solids and Structures* 39 (2002) 6339–6353.
[34] J.N. Reddy, T. Kuppusamy, Natural vibration of laminated anisotropic plates, *Journal of Sound and Vibration* 94 (1984) 63–69.
[35] J.Q. Ye, A three-dimensional free vibration analysis of cross-ply laminated rectangular plates with clamped edges, *Computer Methods in Applied Mechanics and Engineering* 140 (1997) 383–392.
[36] S. Ahmad, B. Irons, O.C. Zienkiewicz, Analysis of thick and thin shell structures by curved finite elements, *International Journal for Numerical Methods in Engineering* 2 (1970) 419–451.

[37] S.J. Lee, S.E. Han, Free-vibration analysis of plates and shells with a nine-node assumed natural degenerated shell element, *Journal of Sound and Vibration* 241 (4) (2001) 605–633.
[38] S. Jayasankar, S. Mahesh, S. Narayanan, Ch. Padmanabhan, Dynamic analysis of layered composite shells using nine node degenerate shell elements, *Journal of Sound and Vibration* 299 (1–2) (2007) 1–11.
[39] H.P. Huttelmaier, M. Epstein, Multilayered finite element formulation for vibration and stability analysis of plates, *ASCE Journal of Engineering Mechanics* 115 (1989) 315–325.
[40] Y. Basar, M.H. Omurtag, Free-vibration analysis of thin/thick laminated structures by layer-wise shell models, *Computers and Structures* 74 (2000) 409–427.
[41] J.L. Mantari, A.S. Oktem, C.Guedes. Soares, A new trigonometric layerwise shear deformation theory for the finite element analysis of laminated composite and sandwich plates, *Computers and Structures* 94–95 (2012) 45–53.
[42] T.S. Plagianakos, E.G. Papadopoulos, Higher-order 2-D/3-D layerwise mechanics and finite elements for composite and sandwich composite plates with piezoelectric layers, *Aerospace Science and Technology* 40 (2015) 150–163.
[43] H. Altenbach, V.A. Eremeyev, K. Naumenko, On the use of the first order shear deformation plate theory for the analysis of three-layer plates with thin soft core layer, *Zeitschrift für angewandte Mathematik und Mechanik* (2015). DOI: http://dx.doi.org/10.1002/zamm.201500069.
[44] M. Weps, K. Naumenko, H. Altenbach, Unsymmetric three-layer laminate with soft core for photovoltaic modules, *Composite Structures* 105 (2013) 332–339.
[45] A. Szekrényes, A special case of parametrically excited systems: Free vibration of delaminated composite beams, *European Journal of Mechanics A/Solids* 49 (2015) 82–105.
[46] M. Di Sciuva, Bending, vibration and buckling of simply supported thick multilayered orthotropic plates: *an evaluation of a new displacement model*, *Journal of Applied Mechanics* 105 (1986) 425–442.
[47] S.D. Kulkarni, S. Kapuria, Free vibration analysis of composite and sandwich plates using an improved discrete Kirchhoff quadrilateral element based on third-order zigzag theory, *Computational Mechanics* 42 (2008) 803–824.
[48] H.D. Chalak, A. Chakrabarti, M.A. Iqbal, A.H. Sheikh, Free vibration analysis of laminated soft core sandwich plates, *Journal of Vibration and Acoustics* 135 (1) (2013) 1–15.
[49] R. Sahoo, B.N. Singh, A new trigonometric zigzag theory for buckling and free vibration analysis of laminated composite and sandwich plates, *Composite Structures* 117 (2014) 316–332.
[50] Y. Frostig, O.T. Thomsen, High-order free vibration of sandwich panels with a flexible core, *International Journal of Solid and Structures* 41 (2004) 1697–1724.
[51] H. Schwarts-Givli, O. Rabinovitch, Y. Frostig, Free vibration of delaminated unidirectional sandwich panels with a transversely flexible core and general boundary conditions a high-order approach, *Journal of Sandwich Structures and Materials* 10 (2) (2008) 99–131.
[52] D. Elmalich, O. Rabinovitch, A high-order finite element for dynamic analysis of soft-core sandwich plates, *Journal of Sandwich Structures and Materials* 14 (5) (2012) 525–555.
[53] V.N. Burlayenko, T. Sadowski, Finite element nonlinear dynamic analysis of sandwich plates with partially detached face sheet and core, *Finite Elements in Analysis and Design* 62 (2012) 49–64.
[54] V.N. Burlayenko, T. Sadowski, Nonlinear dynamic analysis of harmonically excited debonded sandwich plates using finite element modelling, *Composite Structures* 108 (1) (2014) 354–366.
[55] V.N. Burlayenko, T. Sadowski, Transient dynamic response of debonded sandwich plates predicted with finite element analysis, *Meccanica* 49 (11) (2014) 2617–2633.
[56] I. Ivanov, D. Velchev, N. Georgiev, I. Ivanov, Rectangular plate finite element for triplex laminated glass, *Challenging Glass 3: Conference on Architectural and Structural Applications of Glass*, 2012, pp. 679–690.
[57] K. Naumenko, V.A. Eremeyev, A layer-wise theory for laminated glass and photovoltaic panels, *Composite Structures* 112 (1) (2014) 283–291.
[58] J.N. Reddy, A.A. Khdeir, Buckling and vibration of laminated composite plates using various plate theories, *AIAA Journal* 27 (12) (1989) 1808–1817.
[59] W.S. Burton, A.K. Noor, Assessment of computational models for sandwich panels and shells, *Computer Methods in Applied Mechanics and Engineering* 124 (1995) 125–151.
[60] E. Carrera, Theories and finite elements for multilayered plates and shells: *a unified compact formulation with numerical assessment and benchmarking*, *Archives of Computational Methods in Engineering* 10 (3) (2003) 215–296.
[61] M. Aydogdu, Comparison of various shear deformation theories for bending, buckling, and vibration of rectangular symmetric cross-ply plate with simply supported edges, *Journal of Composite Materials* 40 (23) (2006) 2143–2155.
[62] S. Brischetto, R. Torre, Exact 3D solutions and finite element 2D models for free vibration analysis of plates and cylinders, *Curved and Layered Structures* 1 (2014) 59–92.
[63] ABAQUS version 6.9 User's Manual, ABAQUS Inc., Providence, RI 02909-2499, USA, 2010.
[64] V. Birman, C.W. Bert, On the choice of shear correction factor in sandwich structures, *Journal of Sandwich Structures and Materials* 4 (1), 2002, 83-95.
[65] A.W. Leissa, The free vibration of rectangular plates, *Journal of Sound and Vibration* 31 (2) (1973) 257–293.
[66] R.B. Bhat, Natural frequencies of rectangular plates using characteristic orthogonal polynomials in Rayleigh–Ritz method, *Journal Sound and Vibration* 102 (1985) 493–499.
[67] K.M. Liew, K.Y. Lam, S.T. Chow, Free vibration analysis of rectangular plates using orthogonal plate function, *Computers and Structures* 34 (1) (1990) 79–85.
[68] L. Wu, J. Liu, Free vibration analysis of arbitrary shaped thick plates by differential cubature method, *International Journal of Mechanical Sciences* 47 (2005) 63–81.
[69] I. Shufrin, M. Eisenberger, Stability and vibration of shear deformable plates-first order and higher order analyses, *International Journal of Solids and Structures* 42 (2005) 1225–1251.
[70] S. Hurlebaus, L. Gaul, J.T-S. Wang, An exact series solution for calculating the eigenfrequenceis of orthotropic plates with completely free boundary, *Journal of Sound and Vibration* 244 (5) (2001) 747–759.
[71] D.J. Gorman, Accurate free vibration analysis of the completely free orthotropic rectangular plate by the method of superposition, *Journal of Sound and Vibration* 165 (1993) 409–420.
[72] C. Morita, H. Matsuda, T. Sakiyama, T. Hagino, A free vibration analysis of anisotropic rectangular plates with various boundary conditions, *Journal of Sound and Vibration* 187 (5) (1995) 757–770.
[73] J.M. Whitney, N.J. Pagano, Shear deformation in heterogeneous anisotropic plates, *ASME Journal of Applied Mechanics* 37 (1970) 1031–1036.
[74] O.O. Chao, Y.-C. Chern, Comparison of natural frequencies of laminates by 3D theory Part I: *rectangular plates*, *Journal of Sound and Vibration* 230 (5) (2000) 985–1007.
[75] T. Kant, K. Swaminathan, Free vibration of isotropic, orthotropic, and multilayered plates based on higher order refined theory, *Journal of Sound and Vibration* 241 (2) (2001) 319–327.
[76] D.R.J. Owen, Z.H. Li, A refined analysis of laminated plates by finite element displacement methods, II. Vibration and stability, *Computers & Structures* 26 (1987) 915–923.
[77] J. Argyris, L. Tenek, L. Olofsson, Nonlinear free vibration of composite plates, *Computer Methods in Applied Mechanics and Engineering* 115 (1994) 1–51.
[78] M.E. Raville, C.E.S. Veng, Determination of natural frequencies of vibration of a sandwich plate, *Experimental Mechanics* 7 (1967) 490–493.
[79] M. Meunier, R.A. Shenoi, Free vibration analysis of composite sandwich plates, *Proceedings of ImechE, Part C: Journal of Mechanical Engineering* 213 (7) (1999) 715–727.

[80] A.K. Nayak, S.S.J. Moy, R.A. Shenoi, Free vibration analysis of composite sandwich plates based on Reddy's higher-order theory, *Composites: Part B* 33 (2002) 505–519.
[81] K. Malekzadeh, M.R. Khalili, R.K. Mittal, Local and global damped vibrations of plates with a viscoelastic soft flexible core: *an improved high-order approach*, *Journal of Sandwich Structures and Materials* 7 (2005) 431–456.
[82] V.N. Burlayenko, T. Sadowski, Dynamic analysis of debonded sandwich plates with flexible core—numerical aspects and simulation, *Advanced Structured Materials* 15 (2011) 415–440.